NASA/TM–2015-104606 / Vol. 39

Technical Report Series on Global Modeling and Data Assimilation, Volume 39

Randal D. Koster, Editor

Land Boundary Conditions for the Goddard Earth Observing System Model Version 5 (GEOS-5) Climate Modeling System – Recent Updates and Data File Descriptions

Sarith P. Mahanama, Randal D. Koster, Gregory K. Walker, Lawrence L. Takacs, Rolf H. Reichle, Gabrielle De Lannoy, Qing Liu, Bin Zhao, and Max J. Suarez

National Aeronautics and
Space Administration

Goddard Space Flight Center
Greenbelt, Maryland 20771

September 2015

NASA STI Program ... in Profile

Since its founding, NASA has been dedicated to the advancement of aeronautics and space science. The NASA scientific and technical information (STI) program plays a key part in helping NASA maintain this important role.

The NASA STI program operates under the auspices of the Agency Chief Information Officer. It collects, organizes, provides for archiving, and disseminates NASA's STI. The NASA STI program provides access to the NASA Aeronautics and Space Database and its public interface, the NASA Technical Report Server, thus providing one of the largest collections of aeronautical and space science STI in the world. Results are published in both non-NASA channels and by NASA in the NASA STI Report Series, which includes the following report types:

- TECHNICAL PUBLICATION. Reports of completed research or a major significant phase of research that present the results of NASA Programs and include extensive data or theoretical analysis. Includes compilations of significant scientific and technical data and information deemed to be of continuing reference value. NASA counterpart of peer-reviewed formal professional papers but has less stringent limitations on manuscript length and extent of graphic presentations.
- TECHNICAL MEMORANDUM. Scientific and technical findings that are preliminary or of specialized interest, e.g., quick release reports, working papers, and bibliographies that contain minimal annotation. Does not contain extensive analysis.
- CONTRACTOR REPORT. Scientific and technical findings by NASA-sponsored contractors and grantees.
- CONFERENCE PUBLICATION. Collected papers from scientific and technical conferences, symposia, seminars, or other meetings sponsored or co-sponsored by NASA.
- SPECIAL PUBLICATION. Scientific, technical, or historical information from NASA programs, projects, and missions, often concerned with subjects having substantial public interest.
- TECHNICAL TRANSLATION. English-language translations of foreign scientific and technical material pertinent to NASA's mission.

Specialized services also include organizing and publishing research results, distributing specialized research announcements and feeds, providing help desk and personal search support, and enabling data exchange services. For more information about the NASA STI program, see the following:

- Access the NASA STI program home page at http://www.sti.nasa.gov
- E-mail your question via the Internet to help@sti.nasa.gov
- Fax your question to the NASA STI Help Desk at 443-757-5803
- Phone the NASA STI Help Desk at 443-757-5802

NASA/TM–2015-104606/Vol. 39

Technical Report Series on Global Modeling and Data Assimilation,
Volume 39

Randal D. Koster, Editor

Land Boundary Conditions for the Goddard Earth Observing System Model Version 5 (GEOS-5) Climate Modeling System – Recent Updates and Data File Descriptions

Sarith P. Mahanama
Science Systems and Applications, Inc., Lanham, MD

Randal D. Koster
NASA's Goddard Space Flight Center, Greenbelt, MD

Gregory K. Walker
Science Systems and Applications, Inc., Lanham, MD

Lawrence L. Takacs
Science Systems and Applications, Inc., Lanham, MD

Rolf H. Reichle
NASA's Goddard Space Flight Center, Greenbelt, MD

Gabrielle De Lannoy
Universities Space Research Association, Columbia, MD

Qing Liu
Science Systems and Applications, Inc., Lanham, MD

Bin Zhao
Science Systems and Applications, Inc., Lanham, MD

Max J. Suarez
NASA's Goddard Space Flight Center, Greenbelt, MD

National Aeronautics and
Space Administration

Goddard Space Flight Center
Greenbelt, Maryland 20771

September 2015

Level of Review: This material has been technically reviewed by technical management

Abstract

The Earth's land surface boundary conditions in the Goddard Earth Observing System version 5 (GEOS-5) modeling system were updated using recent high spatial and temporal resolution global data products. The updates include: (i) construction of a global 10-arcsec land-ocean-lakes-ice mask; (ii) incorporation of a 10-arcsec Globcover 2009 land cover dataset; (iii) implementation of Level 12 Pfafstetter hydrologic catchments; (iv) use of hybridized SRTM global topography data; (v) construction of the HWSDv1.21-STATSGO2 merged global 30 arc-second soil mineral and carbon data in conjunction with a highly-refined soil classification system; (vi) production of diffuse visible and near-infrared 8-day MODIS albedo climatologies at 30-arcsec from the period 2001-2011; and (vii) production of the GEOLAND2 and MODIS merged 8-day LAI climatology at 30-arcsec for GEOS-5. The global data sets were pre-processed and used to construct global raster data files for the software (mkCatchParam) that computes parameters on catchment-tiles for various atmospheric grids. The updates also include a few bug fixes in mkCatchParam, as well as changes (improvements in algorithms, etc.) to mkCatchParam that allow it to produce tile-space parameters efficiently for high resolution AGCM grids. The update process also includes the construction of data files describing the vegetation type fractions, soil background albedo, nitrogen deposition and mean annual 2m air temperature to be used with the future CatchmentCN model and the global stream channel network to be used with the future global runoff routing model. This report provides detailed descriptions of the data production process and data file format of each updated data set.

CONTENTS

List of Figures

List of Tables

1. INTRODUCTION

In the middle of the last decade, the Catchment Land Surface Model (CLSM: Koster et al, 2000) replaced the Mosaic LSM (Koster et al, 1996) as the Goddard Earth Observing System version 5 (GEOS-5) climate modeling system's land surface model. CLSM calculates surface energy and water budget terms at the Earth's land surface at every model time step and, in so doing, computes surface latent and sensible heat fluxes for the atmospheric model. The use of topographically defined hydraulic catchments as fundamental computational units at the surface instead of quasi-rectangular cells makes the CLSM somewhat unique among macroscale LSMs. The model employs a set of comprehensive state-of-the-art surface hydrologic parameterization schemes that require, at each computational element, surface soil hydraulic properties, land cover type, albedo, and descriptions of vegetation phenology.

When the model was first implemented globally about a decade ago, soil, vegetation, and model parameters at each computational element were derived using the best available global data sets at that time. Below is a description of global data that have been used within the model during the last decade:

1) Simple Biosphere Model 2 land cover classification data from the USGS Global Land Cover Characteristics Data Base Version 2.0 (GLCC v2, 2000) aggregated from 30 arc-second to 2.5 arc-minute;
2) HYDRO1k (GTOPO30, 1996) topography data and 36,716 Level 6 Pfafstetter catchments comprising Earth's land surface;
3) Reynolds (Reynolds et al, 2000) soil texture classes from USGS at 5-arc-minute with GSWP-2 soil hydraulic parameters;
4) AVHRR NDVI-based monthly LAI and greenness fraction climatologies from the period 1982-1998, provided on a $1^{o} \times 1°$grid by GSWP-2 (Dirmeyer and Oki, 2002);
5) MODIS-based VISDF and NIRDF albedo: 16-day climatologies at 1 arc-minute covering the period 2000-2004 (Moody et al., 2008);
6) GSWP-2 (Dirmeyer and Oki, 2002) depth-to-bedrock data on the $1^{o} \times 1°$ grid.

Evolution of the computational power of computers, availability of longer records of higher-resolution global Earth observation data products based on advanced and newer satellite instruments, and more importantly, demand for high resolution modeling and assimilation capabilities (e.g., for the GMAO Nature run and for the SMAP mission) necessitated a comprehensive update of Land surface Boundary Conditions (LBCs) in GEOS-5. These updates include the use of:

1) The GLOBCOVER 2009 (2011) global land cover classification data at 10 arc-second from ESA;
2) 291,284 Level 12 Pfafstetter catchments to comprise the Earth's land surface, along with topography based on a hybrid of SRTM DEM and other best available global data;

3) Merged HWSDv1.21 (HWSD, 2009) and STATSGO2 (NRCS, 2012) soil mineral component and organic carbon data at 30 arc-second;
4) Highly refined soil hydraulic properties from De Lannoy et al. (2014);
5) AVHRR NDVI-based monthly GSWP-2 (Dirmeyer and Oki, 2002) greenness fraction climatology for the period 1982-1998, spatially interpolated from the 1^{o} grid to 30 arc-second;
6) 8-day, 30-arcsec climatology LAI climatology constructed from GEOLAND2 LAI (Baret et al., 2012 and Camacho et al., 2013) and MODIS MOD15A2 v005 LAI;
7) MODIS VISDF and NIRDF (MCD43GF, 2014 and Gao et al., 2014) albedo 8-day climatologies at 30 arc-second for the period 2000-2011; and
8) GSWP-2 (Dirmeyer and Oki, 2002) soil depth-to-bedrock data spatially interpolated from the 1^{o} grid to 30 arc-second.

The Catchment-CN model (Koster et al., 2014), which employs the canopy conductance and carbon physics schemes from NCAR/DOE's Common Land Model Version 4 (CLM4: Oleson et al., 2010), is a recent addition to GMAO modeling capabilities. The Catchment-CN model employs modified CLM land cover types (Catchment-CN types), thereby necessitating the generation of a global dataset of these types. A global stream network using topographically delineated hydrological catchments was also developed.

Again, the base description of the Earth's land surface for GEOS-5 is a mosaic of topographically delineated, irregularly shaped hydrologic catchments. Starting from this description, GEOS-5 uses two different approaches to define the computational elements that are actually used at the land surface. The first approach, typically used when the land model is coupled to the atmospheric model, is to overlay the atmospheric grid onto the mosaic of irregularly shaped hydrologic catchments and then use the atmosphere's regular grid lines to sub-divide any catchments that straddle adjacent atmospheric cells, so that each new (and smaller) land element (or "tile") sees only one overlying atmospheric cell. (See the left panel of Figure 1 for an example of a mosaic of catchments further disaggregated by an overlying atmospheric grid). The second approach is used for select offline CLSM applications. With this approach, the application defines the computational land elements (typically specified to be on a regular grid), and the topography data are derived from the underlying dominant hydrologic catchment, i.e., the irregular catchment that contributes the largest areal fraction to the defined land element. (See the right panel of Figure 1 for one example: the SMAP M36 grid of land surface elements).

The first of the 2-step process that produces LBCs for GEOS-5 involves pre-processing high resolution global data sets, computing climatologies of seasonal variables on native grid pixels, and preparing high resolution global raster files for the mkCatchParam software. The second step involves running the mkCatchParam software to process those raster data files and aggregate variables (or compute dominant vegetation and soil types) to the land model tile space.

The mkCatchParam software produces vegetation type, vegetation dynamic, soil hydraulic, and other model parameters for each computational land element for any given atmospheric grid resolution. For convenience, mkCatchParam also generates global map images of all important parameters and movies of seasonal parameters. The atmospheric grid resolution-specific data

files are typically stored in a subdirectory named “clsm” within BCSDIR of the GEOS-5 experiment. Maps and movies are saved in the “clsm/plots/” directory. The sections below provide detailed descriptions of the data production process and of the file format for each dataset.

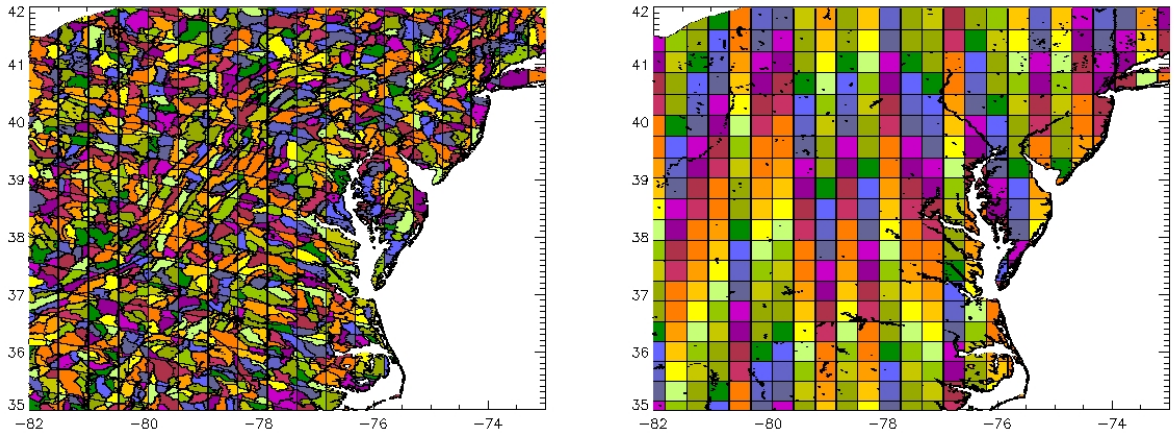

Figure 1: Illustrations of: (left) land surface elements in the northeast United States for the CF0180x6C atmospheric grid, (right) computational grid cells for the SMAP EASEv2 M36 grid.

2. LAND-OCEAN-LAKES-ICE MASKFILE AND CATCHMENT DELINEATION

First, global 30 arc-second GTOPO30 (see GTOPO30, 1996) topography data were re-gridded to 10 arc-second and used to construct a mask at 10 arc-second resolution that contains only 3 surface types: (1) land, (2) lakes, and (3) ocean. Then, glacier locations were overlaid onto the dataset using two data sources: (1) Bedmap2 data (Fretwell et al., 2013) were used over Antarctica and everything south of 65^{o}S latitude; and (2) the Randolph Glacier Inventory (RGI) Version 4 (Arendt et al., 2014) data were used to define glaciers north of 65^{o}S latitude. The next step was to assign each 10 arc-second land pixel to a watershed whose topographic characteristics, namely the statistics of compound topographic index, would be used to parameterize the spatial distribution of soil moisture within catchment-tiles, the computational land elements at the land surface.

In independent work, Verdin (2013) used a hybrid of SRTM data and other existing global DEMs to delineate Level 12 Pfafstetter hydrologic catchments around the world, producing along the way a global 1 arc-minute array of Pfafstetter codes (Verdin and Verdin, 1999). A total of 291,254 independent catchments (each with a unique Pfafstetter code) were defined in Verdin’s data set. The Level 12 Pfafstetter codes are essentially 12-digit numbers, and these large numbers can be computationally challenging to use in catchment-to-grid mapping.

Therefore, for convenience, the Level 12 Pfafstetter codes were sorted in ascending order, and the corresponding catchments were so indexed from 1 to 291,254.

Special attention had to be paid to the 30 catchments with the following Pfafstetter codes:

177552000000,	177553000000,	177554000000,	177555000000,	177561000000,
177562000000,	177563000000,	177564000000,	177591000000,	177592000000,
177593500000,	177593600000,	177642300000,	177644100000,	177646000000,
177647000000,	177648000000,	177649100000,	177660000000,	177678000000,
177681000000,	177682000000,	177691000000,	177692000000,	177793800000,
177793900000,	177794100000,	177795200000,	177796100000,	177890000000.

These 30 catchments are unique in that they straddle the dateline. For logistical reasons, each of these 30 catchments was sub-divided at the dateline into two catchments. Catchment index numbers were then shifted so that the pair would have adjacent numbers, thereby maintaining the ascending order of the Pfafstetter codes. With these additional subdivisions, the Earth's land surface is finally resolved into 291,284 hydrologic catchments. A global 1 arc-minute data array of catchment indices (1-291,284) was constructed and then re-gridded into a 10 arc-second data array.

The constructed land-lakes-ice-ocean mask was further modified to produce the final land-lakes-ice-ocean mask for the GEOS-5 modeling system. The ocean pixels were assigned a value of 0; lake (inland water) pixels were assigned a value of 190000000; and ice pixels were assigned a value of 200000000. The above catchment index array was examined against 10 arc-second land pixels in the mask array, and land pixels were assigned values equal to the corresponding catchment index number. The land pixels that did not have a corresponding catchment index were assigned the catchment index number from the "nearest neighbor" pixel in the catchment index array. The constructed 10 arc-second land-ocean-lakes-ice mask array was saved in the file GEOS5_10arcsec_mask.nc. Note: some of Verdin's catchments were swallowed into lakes, reducing the actual number of hydrologic catchments in the global mask to 290,191.

3. VEGETATION CLASSIFICATION DATA

3.1 Data generation and processing chain

3.1.1 Deriving Mosaic vegetation classes

The Mosaic model (Koster and Suarez, 1996) utilizes 8 vegetation types. The current version of CLSM uses 6 types, with the Mosaic bare soil and desert soil types grouped with Shrubland (Table 1). The reduction in type number is explained by the fact that a shrubland type can be

made to act like a bare soil or desert type simply by assigning an appropriately low value of leaf area index, or LAI, to the surface element. CLSM uses mean seasonal cycles of LAI from global data products (see below), thereby ensuring that bare soil and desert soil behavior will appear in the correct places, and in any case albedos are forced to match those for diffuse radiation in MODIS observations (see below). The absence of the explicit definition of the two bare soil types has an insignificant effect on model behavior.

Global land cover classification at 10-arcsec resolution is available from the European Space Agency (see GLOBCOVER 2009). The first step was to make adjustments to GLOBCOVER 2009 data to match the constructed land-lake-ice-ocean mask in GEOS5_10arcsec_mask.nc in Section 2.0. This ensured land, ocean, lake, and ice pixels in the mask will find similar surface types in the adjusted GLOBCOVER 2009 data array. The land pixels in GLOBCOVER 2009 were made consistent with the mask by assigning the nearest neighbor neighbors land cover type for the missing and mismatching land pixels in GLOBCOVER 2009 and the modified GLOBCOVER 2009 data array was saved in ESAGlobalCover.nc.

Table 1 shows the mapping scheme employed to convert, at each 10-arcsec pixel, an ESA land cover type in ESAGlobalCover.nc into a Mosaic land cover type(s). The Mosaic types used for catchment surface elements are determined by computing the dominant Mosaic type of all 10-arcsec pixels within the catchment in question (Figure 2).

ESA land cover type	Corresponding Mosaic land cover type
11	4
14	4
20	4
30	4
40	1
50	2
60	2
70	3
90	3
100	2 (50%) and 3 (50%)
110	2 (30%), 5 (30%), and 4 (40%)
120	2 (20%), 5 (20%), and 4 (60%)
130	5
140	4

150	inside 50°S and 50°N lats: 4 (50%) and 5 (50%) outside of 50°S and 50°N lats: 4 (50%) and 6 (50%)
160	inside 20°S and 20°N lats: 1 outside of 20°S and 20°N lats: 2
170	1
180	4
190	4
200	5

Table 1: ESA to Mosaic mapping: The reader is referred to Table 2 of GLOBCOVER 2009 (2011) for a detailed description of ESA land cover types. The 6 Mosaic land cover types are: 1 (Broadleaf Evergreen), 2 (Broadleaf Deciduous), 3 (Needleleaf), 4 (Grassland), 5 (Broadleaf Shrubs), and 6 (Dwarf trees).

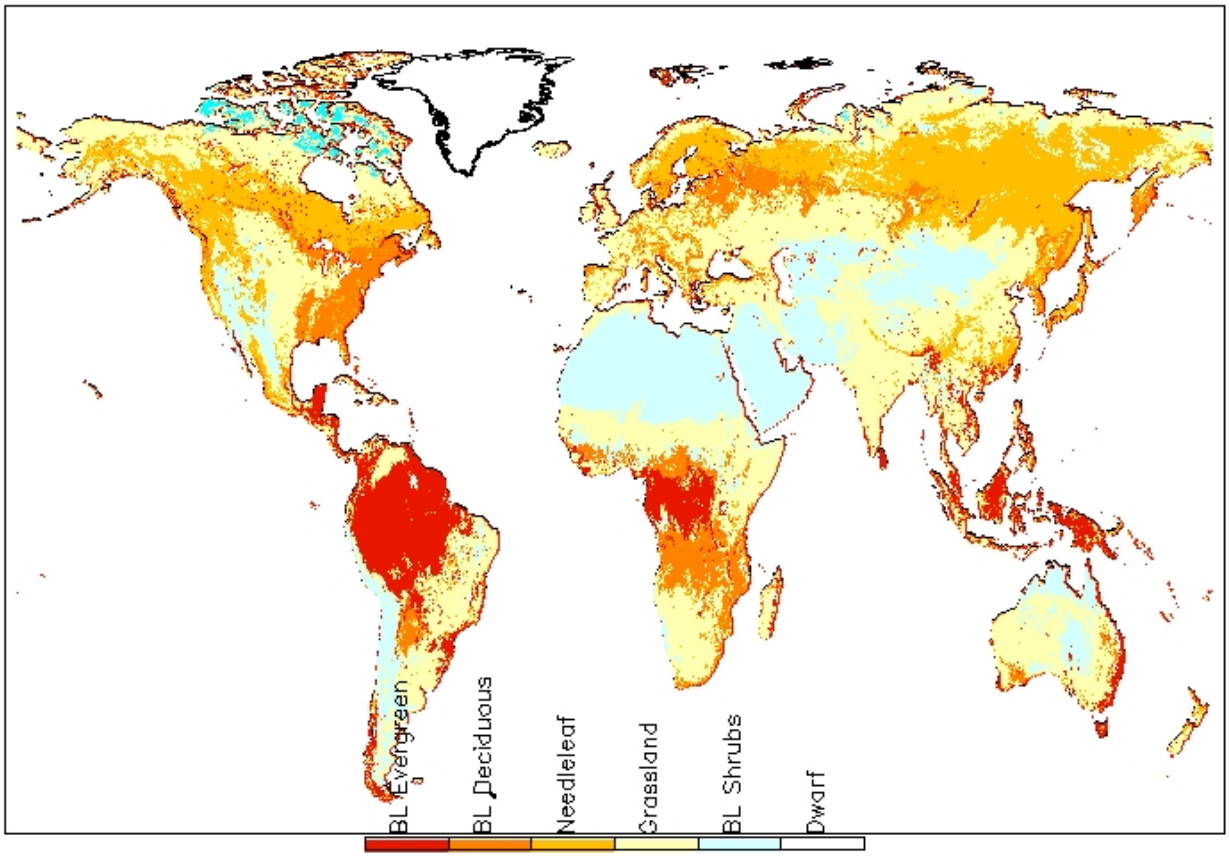

Figure 2: Mosaic vegetation classes.

3.1.2 Deriving Catchment-CN classes

The Common Land Model version 4 (CLM4: Oleson et al., 2010) utilizes 17 vegetation classes (Table 2). A global array of fractional coverage of each of the 17 classes on a 1152x768 grid, as used by CLM4 was obtained from UCAR.

The Catchment-CN model's vegetation classification is based on that used by CLM4, with fractional coverage of each type derived from the Global ESA land cover classification. Each ESA type was mapped into one or more of the CLM4 types. For instance, ESA crop types were mapped one-to-one into CLM4's crop type, whereas ESA mosaic vegetation was fractionally mapped into region-appropriate grass, shrub, and forest types. This fractional mapping was based on the relative fractions found in the original 1152x768 CLM4 gridded arrays and on latitude (for differentiating certain types, such as Arctic c3 grass). Bare soil from the ESA land cover classification is mapped into the broadleaf deciduous shrub type, since bare soil is not an allowed type in our implementation.

For Catchment-CN, the stress deciduous types (crop and temperate shrubs/grass) utilized by CLM4 is replaced by a mix of two sub-types, one that is seasonally deciduous (with a daylight trigger) and one that is not. Both sub-types are subject to moisture stress triggers but not to temperature (freezing) stress triggers. The removal of the temperature stress trigger eliminated unnatural swings in leaf carbon during brief temperature stress senescence (Koster et al. 2014). The relative fractions of the two sub-types applied vary linearly with latitude between 32°-42° in both hemispheres, with 100% of the stress deciduous type being replaced by the seasonally deciduous sub-type at 42° and 100% replaced by the non-seasonally deciduous type at 32°.

Within each surface element, the two dominant types are identified; the remaining types are ignored. (Note, however, that in the latitude band 32°-42°, the presence of two sub-types for a potentially dominant type implies that up to four sub-types may be followed.) The vegetation fractions for the two dominant types are scaled so that they sum to one. Figure 3 shows global maps of primary and secondary Catchment-CN types.

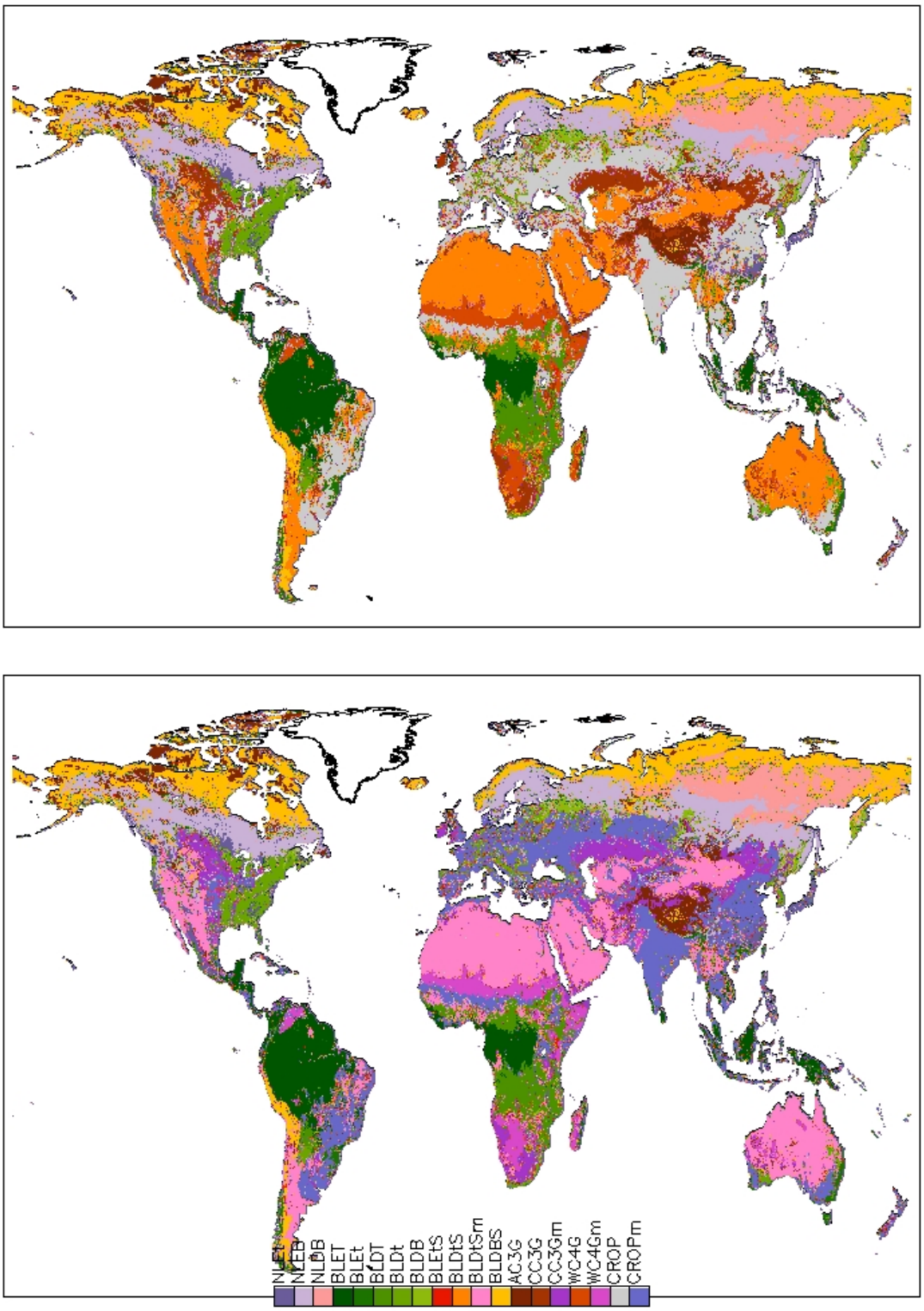

Figure 3: Catchment-CN (top) primary vegetation types, and (bottom) secondary vegetation types.

Land cover	CLM Class	Catchment-CN Class	Map Legend (Figure 3)
Bare	1	NA	BARE
Needleleaf evergreen temperate tree	2	1	NLEt
Needleleaf evergreen boreal tree	3	2	NLEB
Needleleaf deciduous boreal tree	4	3	NLDB
Broadleaf evergreen tropical tree	5	4	BLET
Broadleaf evergreen temperate tree	6	5	BLEt
Broadleaf deciduous tropical tree	7	6	BLDT
Broadleaf deciduous temperate tree	8	7	BLDt
Broadleaf deciduous boreal tree	9	8	BLDB
Broadleaf evergreen temperate shrub	10	9	BLEtS
Broadleaf deciduous temperate shrub	11	10	BLDtS
Broadleaf deciduous temperate shrub [moisture stress only]	NA	11	BLDtSm
Broadleaf deciduous boreal shrub	12	12	BLDBS
Arctic c3 grass	13	13	AC3G
Cool c3 grass	14	14	CC3G
Cool c3 grass [moisture stress only]	NA	15	CC3Gm
Warm c4 grass	15	16	WC4G
Warm c4 grass [moisture stress only]	NA	17	WC4Gm
Crop	16	18	CROP
Crop [moisture stress only]	NA	19	CROPm
Water	17	NA	

Table 2: CLM and Catchment-CN land cover classification description.

3.1.3 Deriving Nitrogen Deposition, Annual mean 2m Air Temperature, and Soil background albedo for the Catchment-CN Model

Nitrogen deposition data used in CLM4 (Oleson et al., 2010) were obtained from UCAR. The approximately quarter degree CLM4 deposition data (sum of NHx and NOx species) were spatially interpolated to catchment surface elements and saved (with units of ng m-2 s-1) in the "CLM_NDep_SoilAlb_T2m" file (Figure 4, top panel). Note that the units of the input deposition data in the Catchment-CN model is g m-2 s-1, and thus the values in the file must be scaled by 1.e-9 before using inside the model.

The Catchment-CN phenology routine computes a "growing degree day" summation to determine when seasonal and stress deciduous plant functional types (PFT) become active. The critical value for this summation is a function of annual mean 2m air temperature. CLM4 uses the previous year's annual mean 2m air temperature (K). In the Catchment-CN model, however, we instead use the climatological annual mean 2m air temperature. Two sources of multi-year global hydrometeorological forcing were used to compute climatological annual mean 2m air temperature separately: 1) GMAO MERRA-2, hourly, 0.625^{o}x0.5^{o} resolution, data from the period 1980-2014, and 2) Sheffield et al (2006), 3-hourly, 1-degree data from the period 1948-2012. The climatological means were computed on the native forcing grids (see middle and bottom panels in Figure 4), then spatially interpolated to catchment surface elements, and finally saved in the file "CLM_NDep_SoilAlb_T2m".

In areas of low LAI (less than one), surface albedo in the Catchment-CN model is prescribed using MODIS soil background albedo. For LAI=0, the soil background albedo has full weight; at LAI=1, the albedo is fully determined by mapped catchment vegetation type (using subroutine SIBALB). A linear ramp is used to weight between the MODIS soil background albedo and the SIBALB albedo for 0<LAI<1. There are four albedo components: visible direct (VISDR), visible diffuse (VISDF), near-infrared direct (NIRDR), and near-infrared diffuse (NIRDF). Global fields of soil background VISDR, VISDF, NIRDR and NIRDF at 3-arcmin resolution were obtained from Houldcroft et al. (2009) and spatially aggregated to catchment surface elements for the Catchment-CN model (Figure 5).

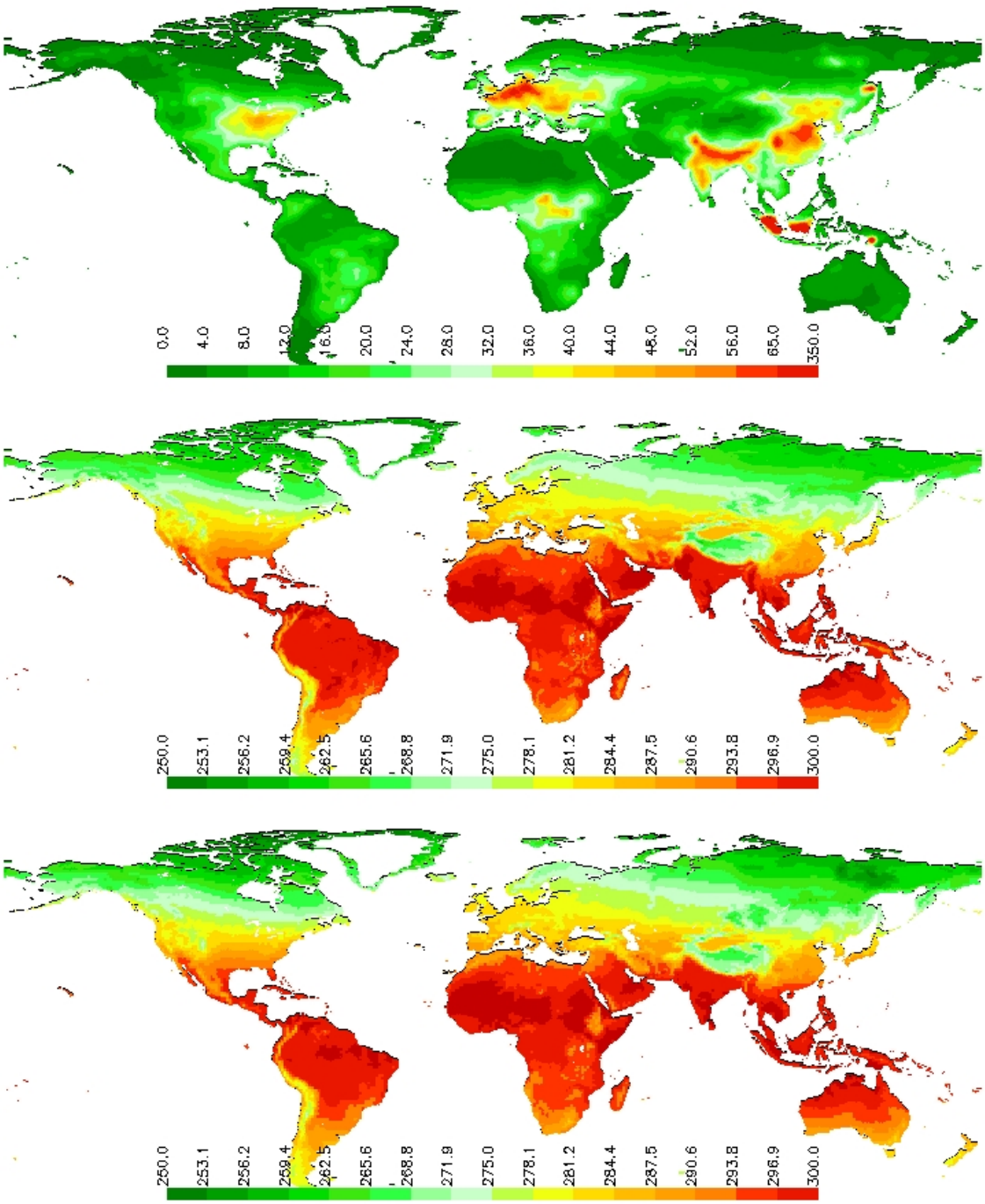

Figure 4: (top) Nitrogen deposition (sum of NHx and NOx species) [ng m^{-2} s^{-1}], (middle) Mean annual 2m air temperature from MERRA-2 [K] for the period 1980-2014, (bottom) Mean annual 2m air temperature from Sheffield et al. (2006) data [K] for the period 1948-2012.

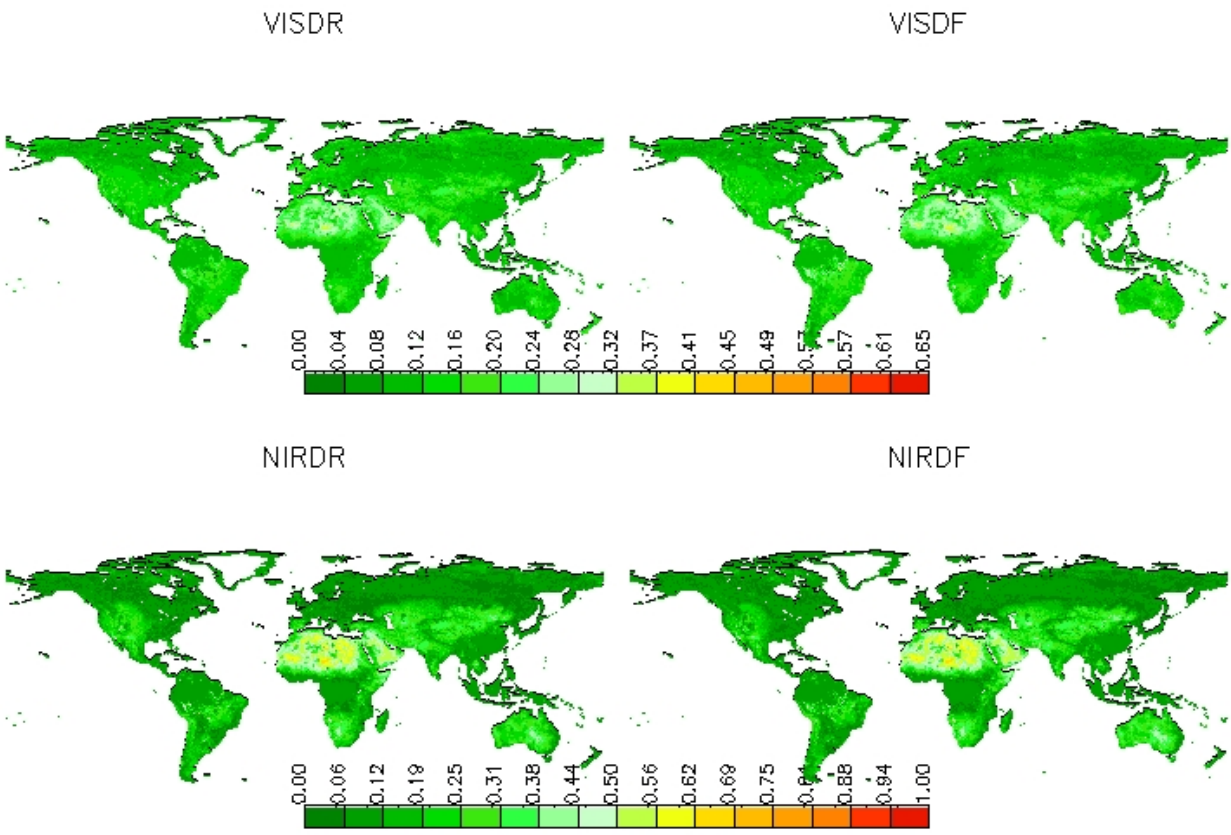

Figure 5: Global maps of Houldcroft et al. (2009) soil background albedo data [-].

3.1.4 Deriving Canopy Height Data

Global 30-arcsec canopy height data, used (in some implementations) in the calculation of surface roughness, were obtained from NASA's Jet Propulsion Laboratory (Simrad et al., 2011). These heights were spatially aggregated to catchment surface elements (Figure 6).

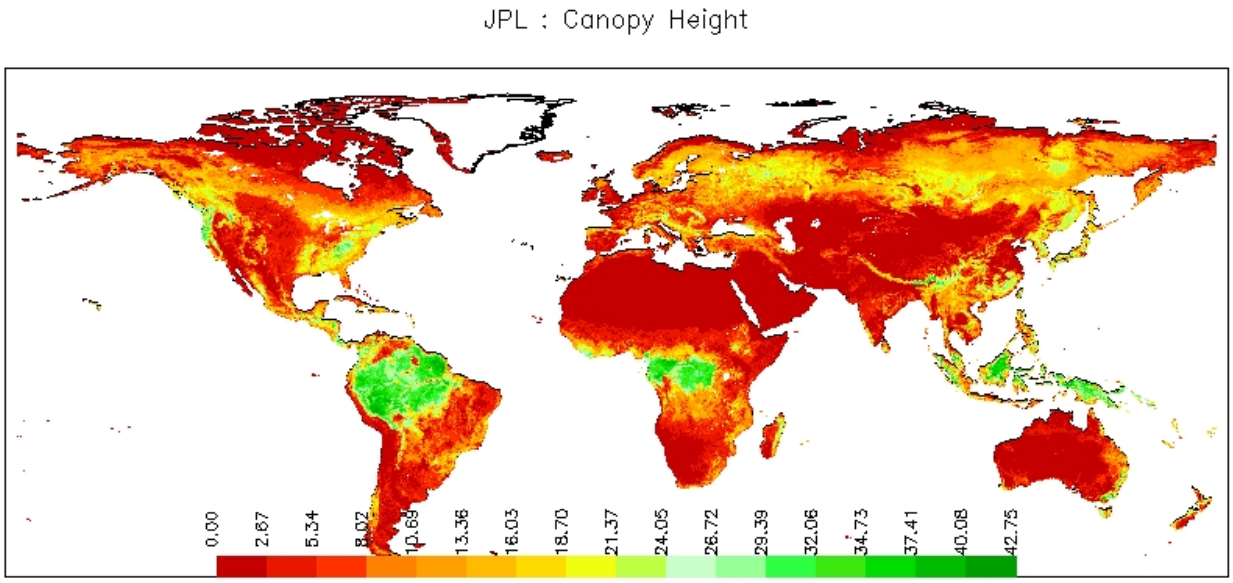

Figure 6: Map of canopy height data [m].

3.2 Data files and images

3.2.1 Mosaic vegetation types and fractions

```
file name: mosaic_veg_typs_fracs

do n = 1, NTILES
     read(10,*'')       tile_index,pfaf_code,
     primary_veg_type, secondary_veg_type,
     primary_veg_frac,  secondary_veg_frac, canopy_height
end do

where for each tile:

tile_index [-]          Tile Number
pfaf_code [-]           catchment index (1-291284) after
                        sorting Pfafstetter codes in
                        ascending order
primary_veg_type [-]    primary vegetation type
secondary_veg_type [-]  secondary vegetation type
primary_veg_frac [-]    primary vegetation fraction
secondary_veg_frac [-]  secondary vegetation fraction
canopy_height [m]       canopy height
```

3.2.2 CLM and Catchment-CN vegetation types and fractions

```
file name: CLM_veg_typs_fracs

do n = 1, NTILES
read (10,'(2I8,4I3,4f7.2,2I3,2f7.2)')    &
     tile_index,pfaf_code,                    &
     CLM-C_pt1,CLM-C_pt2,CLM-C_st1,CLM-C_st2, &
     CLM-C_pf1,CLM-C_pf2,CLM-C_sf1,CLM-C_sf2, &
     CLM_pt, CLM_st, CLM_pf, CLM_sf
enddo

Where for each tile:


tile_index [-]  Tile Number
pfaf_code [-]   catchment index (1-291284) after sorting
                Pfafstetter codes in ascending order
CLM-C_pt1 [-]   Catchment-CN primary type 1
CLM-C_pt2 [-]   Catchment-CN primary type 2 (if sub-types
                exist, in 32°-42° latitudinal band)
CLM-C_st1 [-]   Catchment-CN secondary type 1
CLM-C_st2 [-]   Catchment-CN secondary type 2 (if sub-types
                exist, in 32°-42° latitudinal band)
CLM-C_pf1 [-]   Catchment-CN fraction of 1st primary type
CLM-C_pf2 [-]   Catchment-CN fraction of 2nd primary type
                (if sub-types exist, in 32°-42° latitudinal
                band)
CLM-C_sf1 [-]   Catchment-CN fraction of 1st secondary type
CLM-C_sf2 [-]   Catchment-CN fraction of 2nd secondary type
                (if sub-types exist, in 32°-42° latitudinal
                band)
CLM_pt [-]      CLM primary type
CLM_st [-]      CLM secondary type
CLM_pf [-]      CLM fraction of primary type
CLM_sf [-]      CLM fraction of secondary type
```

3.2.3 Nitrogen Deposition, Annual mean 2m Air Temperature, and Soil background albedo for the Catchment-CN Model

```
file name: CLM_NDep_SoilAlb

do n = 1, NTILES
read (10,'(f10.4,4f7.4,2f8.3)')    &
```

```
     NDEP,VISDR, VISDF, NIRDR, NIRDF, T2_M, T2_S
enddo

Where for each tile:


NDEP [ng m-2 s-1]  Nitrogen deposition
VISDR [-]          Direct visible soil background albedo
VISDF [-]          Diffuse visible soil background albedo
NIRDR [-]          Direct near-infrared soil background
                   albedo
NIRDF [-]          Diffuse near-infrared soil background
                   albedo
T2_M [K]           Mean annual 2m air temperature from MERRA-
                   2 (averaged over 1980-2014)
T2_S [K]           Mean annual 2m air temperature from
                   Sheffield et al. (2006) (averaged over
                   1980-2014)
```

4. TOPOGRAPHY AND SOIL DATA

4.1 Data generation and processing chain

Verdin (2013) produced global 1-arcmin raster arrays of Compound Topographic Index (CTI) statistics: mean, standard deviation and skewness. As described in Section 2, Verdin (2013) also delineated the Earth's land surface into 291,254 hydrologic catchments, and sub-dividing 30 dateline catchments increased the total number of catchments to 291,284. Furthermore, Verdin (2013) produced an associated global 1 arc-minute raster array of Level 12 Pfafstetter codes to map those hydrologic catchments. The 1 arc-minute data array was also updated to accommodate the changes stemming from the 30 dateline catchments.

The following approach was employed to derive statistics of CTI for each of the 291,284 catchment using the available CTI statistics at 1 arc-minute resolution. First, the N pixels belonging to a given catchment were identified. For each of these pixels, a 5000-element array of sample CTIs was constructed using a 3-parameter gamma distribution; the 5000-element array was constructed so as to have the same mean, standard deviation, and skewness as was identified for the pixel in the Verdin (2013) dataset. If the Verdin (2013) data did not provide a skewness value for the pixel, a Gaussian distribution was used to construct the 5000-element CTI array.

Second, the 5000 elements from each of the N pixels making up the given catchment were combined to form a single, 5000 x N-element array of CTIs. Finally, the mean, standard

deviation, and skewness of the CTI values in this single larger array were computed and assigned to the catchment. Figure 4 shows the resulting global maps of catchment-level CTI statistics.

The user is referred to De Lannoy et al. (2014) for a complete description of the procedure used to generate our global datasets of soil type. The basis of the datasets is a merging of STATSGO2 (NRCS, 2012) data with the Harmonized World Soil Data (HWSD, 2009) version 1.21 dataset, with special techniques employed to fill data gaps. The merging process produced global arrays of sand, clay and organic matter percentages at 30 arc-second resolution for two soil layers: 0-30cm and 30-100cm. From these data, De Lannoy et al. (2014) defined 253 soil classes, and from these classes they derived soil hydraulic properties for the surface and profile layers, separately (Table 3). The representative (and thus utilized) soil type for a given hydrological catchment was determined through a somewhat complex procedure developed by De Lannoy et al. (2014); the upshot of the procedure is that the chosen type actually appears within the catchment and has, compared to all of the 30 arc-second pixels in the catchment, roughly median texture percentages. The surface soil hydraulic properties for the 253 classes appear in Table 3. See Figure 5 for corresponding global maps of soil hydraulic properties.

The Second Global Soil Wetness Project (Dirmeyer, and Oki, 2002) provided a global, 1-degree dataset of soil depth to bedrock. The GSWP-2 soil depth data were spatially interpolated onto 30-arcsec pixels. The interpolated soil depth data were averaged across a given catchment land element to determine that catchment's effective soil depth.

4.2 Data files and images

4.2.1 Tile types, location, area and Pfafstetter catchment mapping

file name: BCSDIR/BCRSLV/BCRSLV-Pfafstetter.til
The 8-line header contains: (line 1) N_GLOBAL, number of columns in the global raster array of tile indices, number of rows in the global raster array of tile indices; (line 2) "2" depicts that all land, ocean, lakes, and ice tiles are included in the table below; (line 3) locations of the poles (PE is for pole edge grid, and PC is pole center grids), grid resolution and location of the dateline for finite volume atmospheric grids (CF for cube-sphere grids; DE is for finite element grids with the dateline at the western edge of the grid, and DC is for finite element grids with the dateline lying along the center of the first column); (line 4) number of columns in the atmospheric grid (AGCM_IM); (line 5) number of rows in the atmospheric grid (AGCM_JM); (line 6) locations of the poles (PE or PC), grid resolution and location of the dateline (DE or DC)for the ocean grid ; (line 7) number of columns in the ocean grid (OGCM_IM); and (line 8) number of rows in the ocean grid (OGCM_JM). The 8-line header is followed by a table that

has N_GLOBAL number of rows containing tile geographic information for each tile separately.

```
do n = 1,N_GLOBAL  !(including ocean, glaciers, and lakes)
     read (10,*)type, area, longitude, latitude, &
     ig, jg, cell_frac, pfaf_index, pfaf_code, pfaf_frac
end do
```

Note: the below description is valid only for the land block of the table, i.e. for rows whose surface type is 100 in the first column. The ocean, lakes and ice tiles have their own indexing and tile specific fractions while the format of the read statement remains unchanged.

For each tile:

type [-]	tile type (100-land; 0-ocean; 19-lakes; 20-ice)
longitude [degree]	longitude at the centroid of the tile
latitude [degree]	latitude at the centroid of the tile
ig [-]	i-index of the AGCM grid cell where the tile is located (1 - AGCM_IM)
jg [-]	j-index of the AGCM grid cell where the tile is located (1 – AGCM_JM)
pfaf_index[-]	catchment index (1-291,284) after sorting Pfafstetter codes in ascending order
cell_frac [-]	fraction of the AGCM grid cell covered by the tile
pfaf_frac [-]	fraction of the Pfafstetter catchment covered by the tile

4.2.2 Western, eastern, southern, and northern edges and mean elevation of tiles

file name: catchment.def

```
read (10,*) NTILES
do n = 1, NTILES
     read (10,'(i8,i8,5(2x,f9.4))') tile_index,pfaf_index,
          min_lon,max_lon,min_lat,max_lat, mean_elevation )
end do
```

where for each tile:

tile_index [-]	Number
pfaf_index [-]	catchment index (1-291,284) after

```
                        sorting Pfafstetter codes in ascending
                        order
     min_lon [degree]   Westernmost edge of tile
     max_lon [degree]   Easternmost edge of tile
     min_lat [degree]   Southernmost edge of tile
     max_lat [degree]   Northernmost edge of tile
     mean_elevation [m] area-averaged elevation of tile
```

4.2.3 Tile topography - statistics of Compound Topographic Index (CTI)

```
     file name: cti_stats.dat

     read (10,*) NTILES
     do n = 1, NTILES
          read  (10,'(i8,i8,5(1x,f8.4))')  tile_index,pfaf_index,
&
          cti_mean, cti_std, cti_min, cti_max, cti_skew
     end do

     where for each tile:

     tile_index        Number [-]
     pfaf_index        catchment index (1-291284) after sorting
                       Pfafstetter codes in ascending order [-]
     cti_mean          mean CTI of the underlying hydrologic
                       catchment [log(m)]
     cti_std           standard deviation of CTI of the
                       underlying hydrologic catchment
     cti_min           minimum CTI value in the underlying
                       hydrologic catchment
     cti_max           maximum CTI value in the underlying
                       hydrologic catchment
     cti_skew          skewness of CTI of the underlying
                       hydrologic catchment
```

4.2.4 Soil Parameters

```
     file name: soil_param.dat

     do n = 1, NTILES
     read   (10,'(i8,i8,i4,i4,3f8.4,f12.8,f7.4,f10.4,3f7.3,4f7.3,
&
          2f10.4)') tile_index, pfaf_code, soil_class_top, &
          soil_class_com, BEE, PSIS, POROS, COND, WPWET,   &
          soildepth, gravel, OrgCarbon_top, OrgCarbon_rz,  &
```

```
      sand_top, clay_top, sand_rz, clay_rz, WPWET_top, &
      POROS_top
 end do
```

where for each tile:

tile_index [-]	Number
pfaf_index [-]	catchment index (1-291,284) after sorting Pfafstetter codes in ascending order
soil_class_top [-]	soil class for the surface layer (0-30cm)
soil_class_com [-]	soil class for the root-zone layer (0-100cm)
BEE [-]	b-parameter of the tension curve
PSIS [m H2O]	air entry pressure for the root-zone (matric potential)
POROS [m3/m3]	soil moisture content at saturation for the root-zone
COND (m/s)	saturated hydraulic conductivity at the surface
WPWET [-]	ratio of wilting point to porosity for the root-zone
soildepth [mm]	depth to bedrock
gravel [vol%]	percentage of gravel in the surface layer (0-30cm)
OrgCarbon_top [w%]	percentage of organic carbon in the surface layer (0-30cm)
OrgCarbon_rz [w%]	percentage of organic carbon in the root zone (0-100cm)
sand_top [w%]	percentage of sand in the surface layer (0-30cm)
clay_top [w%]	percentage of clay in the surface layer (0-30cm)
sand_rz [w%]	percentage of sand in the root-zone layer (0-100cm)
clay_rz [w%]	percentage of clay in the root-zone layer (0-100cm)
WPWET_top [-]	ratio of wilting point to porosity for the surface layer (0-30cm)
POROS_top [m3/m3]	soil moisture content at saturation in the surface layer (0-30cm)

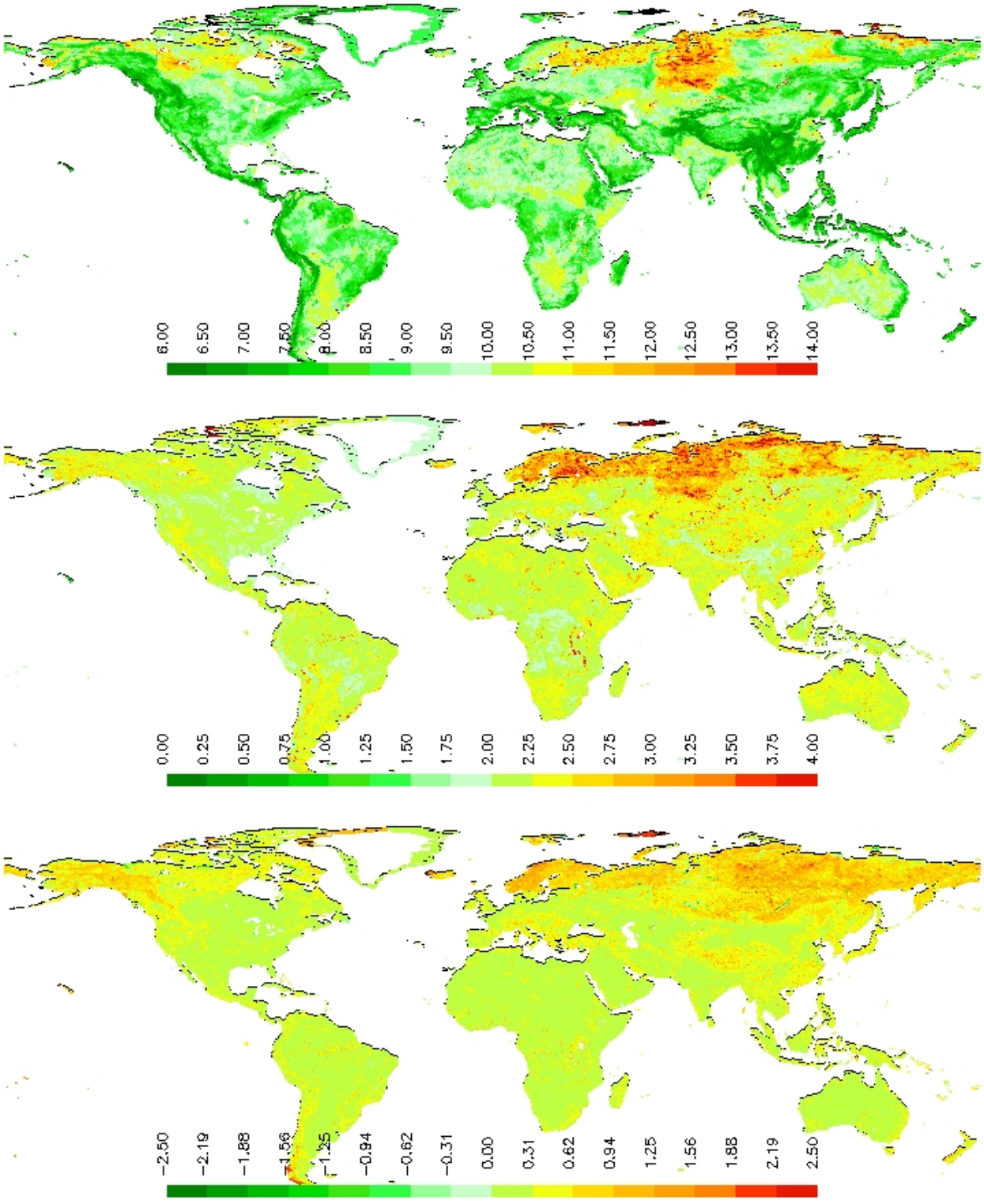

Figure 7: (top) Mean of Compound Topographic Index (CTI) in catchment space, (middle) standard deviation of CTI, and (bottom) skewness of CTI.

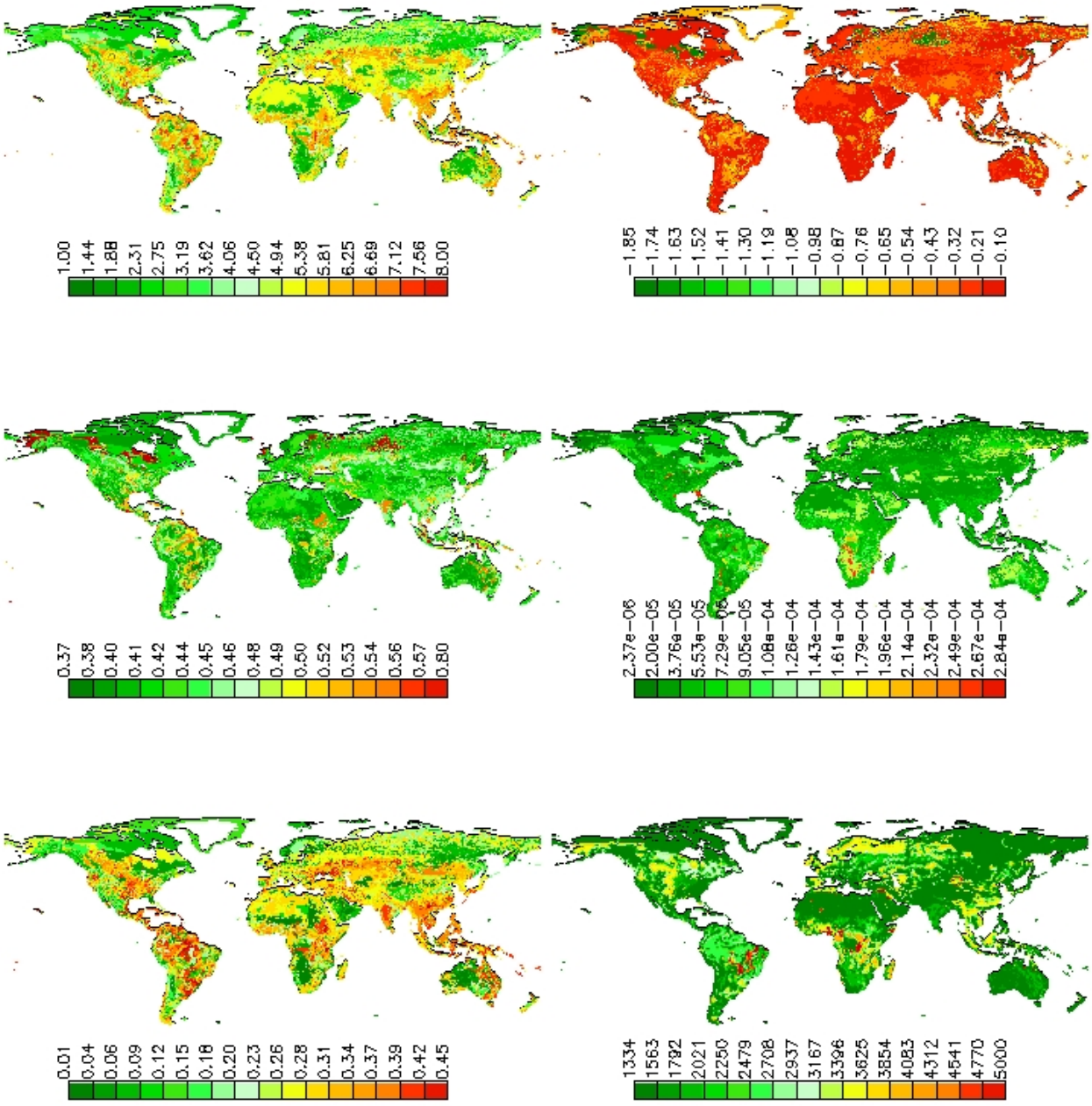

Figure 8 : Select soil hydraulic parameters for the CF0360x6C model tile space: (top left) b parameter (the parameter describing the shape of the water retention curve), (top right) air entry pressure, ψ_s (m H_20), (middle left) porosity (m^3/m^3), (middle right) hydraulic conductivity (ms^{-1}) at the surface, (bottom left) wilting point wetness (-), and (bottom right) soil depth-to-bedrock (mm).

Class	Cl	Sa	OC	θ_s^*	ρ_b	θ_s	b	Ψ_s	K_s	wp	fc
	[w%]	[w%]	[w%]	[m^3/m^3]	[g/cm^3]	[m^3/m^3]	[-]	[m]	[m/s]	[m^3/m^3]	[m^3/m^3]
1	53.33	43.33	0.26	0.47	1.32	0.47	4.94	-0.28	2.10E-05	0.130	0.28
2	56.67	36.67	0.26	0.49	1.26	0.50	5.41	-0.40	1.42E-05	0.165	0.33
3	53.33	33.33	0.26	0.48	1.27	0.50	6.21	-0.37	9.85E-06	0.189	0.35
4	56.67	26.67	0.26	0.50	1.21	0.52	6.01	-0.54	8.84E-06	0.205	0.39
5	53.33	23.33	0.26	0.50	1.22	0.52	6.33	-0.50	7.34E-06	0.211	0.39
6	56.67	16.67	0.26	0.52	1.16	0.55	5.91	-0.74	6.84E-06	0.222	0.42
7	53.33	13.33	0.26	0.52	1.17	0.54	6.08	-0.67	5.81E-06	0.222	0.42
8	56.67	6.67	0.26	0.54	1.10	0.57	5.54	-1.00	5.45E-06	0.228	0.45
9	53.33	3.33	0.26	0.54	1.12	0.56	5.66	-0.90	4.56E-06	0.225	0.44
10	43.33	53.33	0.26	0.43	1.43	0.42	5.02	-0.15	2.09E-05	0.107	0.23
11	46.67	46.67	0.26	0.44	1.38	0.45	5.81	-0.19	1.41E-05	0.143	0.28
12	43.33	43.33	0.26	0.44	1.38	0.45	6.42	-0.20	9.60E-06	0.161	0.29
13	46.67	36.67	0.26	0.46	1.33	0.48	6.60	-0.26	8.61E-06	0.181	0.32
14	43.33	33.33	0.26	0.46	1.34	0.47	6.68	-0.27	7.01E-06	0.183	0.32
15	46.67	26.67	0.26	0.48	1.29	0.49	6.66	-0.35	6.56E-06	0.198	0.35
16	43.33	23.33	0.26	0.47	1.30	0.49	6.57	-0.36	5.45E-06	0.195	0.35
17	46.67	16.67	0.26	0.49	1.24	0.51	6.43	-0.46	5.15E-06	0.208	0.38
18	43.33	13.33	0.26	0.49	1.25	0.50	6.30	-0.47	4.21E-06	0.201	0.37
19	46.67	6.67	0.26	0.51	1.19	0.53	6.07	-0.61	3.97E-06	0.212	0.40
20	43.33	3.33	0.26	0.50	1.21	0.52	5.93	-0.60	3.15E-06	0.204	0.39
21	33.33	63.33	0.26	0.40	1.50	0.39	4.45	-0.11	2.13E-05	0.077	0.18
22	36.67	56.67	0.26	0.41	1.47	0.41	5.41	-0.13	1.40E-05	0.112	0.23
23	33.33	53.33	0.26	0.41	1.47	0.42	5.77	-0.14	9.41E-06	0.125	0.24
24	36.67	46.67	0.26	0.43	1.43	0.43	6.23	-0.17	8.31E-06	0.146	0.27
25	33.33	43.33	0.26	0.42	1.44	0.43	6.09	-0.19	6.64E-06	0.145	0.27
26	36.67	36.67	0.26	0.44	1.40	0.45	6.39	-0.23	6.16E-06	0.163	0.30
27	33.33	33.33	0.26	0.44	1.40	0.45	6.08	-0.26	5.02E-06	0.157	0.29
28	36.67	26.67	0.26	0.45	1.36	0.46	6.29	-0.31	4.72E-06	0.173	0.32
29	33.33	23.33	0.26	0.45	1.37	0.46	5.92	-0.34	3.77E-06	0.164	0.31
30	36.67	16.67	0.26	0.46	1.32	0.48	6.06	-0.40	3.56E-06	0.179	0.34
31	33.33	13.33	0.26	0.46	1.34	0.47	5.68	-0.44	2.75E-06	0.168	0.33
32	36.67	6.67	0.26	0.48	1.28	0.49	5.76	-0.51	2.59E-06	0.182	0.35
33	33.33	3.33	0.26	0.47	1.30	0.48	5.39	-0.56	1.93E-06	0.170	0.34
34	23.33	73.33	0.26	0.39	1.54	0.37	3.45	-0.10	2.28E-05	0.045	0.14
35	26.67	66.67	0.26	0.39	1.52	0.39	4.41	-0.11	1.45E-05	0.075	0.18
36	23.33	63.33	0.26	0.39	1.52	0.40	4.55	-0.13	9.59E-06	0.084	0.19
37	26.67	56.67	0.26	0.40	1.50	0.41	5.15	-0.15	8.21E-06	0.106	0.22
38	23.33	53.33	0.26	0.40	1.50	0.41	4.87	-0.18	6.45E-06	0.102	0.22
39	26.67	46.67	0.26	0.41	1.48	0.42	5.36	-0.20	5.84E-06	0.121	0.25
40	23.33	43.33	0.26	0.41	1.48	0.42	4.94	-0.24	4.66E-06	0.112	0.24
41	26.67	36.67	0.26	0.42	1.45	0.43	5.34	-0.27	4.30E-06	0.130	0.27

42	23.33	33.33	0.26	0.42	1.46	0.42	4.87	-0.32	3.37E-06	0.119	0.26
43	26.67	26.67	0.26	0.43	1.42	0.44	5.22	-0.35	3.13E-06	0.136	0.28
44	23.33	23.33	0.26	0.42	1.44	0.43	4.72	-0.43	2.37E-06	0.124	0.28
45	26.67	16.67	0.26	0.44	1.40	0.44	5.03	-0.46	2.21E-06	0.140	0.30
46	23.33	13.33	0.26	0.43	1.41	0.44	4.54	-0.56	1.61E-06	0.127	0.29
47	26.67	6.67	0.26	0.45	1.37	0.45	4.80	-0.59	1.49E-06	0.142	0.31
48	23.33	3.33	0.26	0.44	1.39	0.44	4.33	-0.71	1.04E-06	0.128	0.31
49	13.33	83.33	0.26	0.40	1.52	0.37	2.38	-0.11	2.67E-05	0.018	0.09
50	16.67	76.67	0.26	0.39	1.53	0.38	3.17	-0.12	1.61E-05	0.039	0.13
51	13.33	73.33	0.26	0.39	1.52	0.39	3.19	-0.15	1.05E-05	0.044	0.15
52	16.67	66.67	0.26	0.39	1.52	0.39	3.77	-0.15	8.57E-06	0.063	0.17
53	13.33	63.33	0.26	0.39	1.52	0.39	3.46	-0.20	6.63E-06	0.058	0.17
54	16.67	56.67	0.26	0.40	1.52	0.40	3.97	-0.21	5.76E-06	0.076	0.20
55	13.33	53.33	0.26	0.39	1.52	0.40	3.55	-0.27	4.51E-06	0.067	0.20
56	16.67	46.67	0.26	0.40	1.51	0.40	4.01	-0.28	4.02E-06	0.084	0.22
57	13.33	43.33	0.26	0.40	1.51	0.40	3.54	-0.37	3.08E-06	0.073	0.21
58	16.67	36.67	0.26	0.40	1.50	0.41	3.97	-0.39	2.79E-06	0.090	0.24
59	13.33	33.33	0.26	0.40	1.51	0.40	3.48	-0.51	2.06E-06	0.078	0.23
60	16.67	26.67	0.26	0.41	1.48	0.41	3.86	-0.52	1.88E-06	0.094	0.25
61	13.33	23.33	0.26	0.40	1.50	0.40	3.38	-0.69	1.33E-06	0.081	0.25
62	16.67	16.67	0.26	0.41	1.47	0.41	3.73	-0.69	1.22E-06	0.097	0.27
63	13.33	13.33	0.26	0.41	1.49	0.41	3.25	-0.92	8.30E-07	0.084	0.27
64	16.67	6.67	0.26	0.42	1.45	0.42	3.57	-0.91	7.60E-07	0.099	0.29
65	13.33	3.33	0.26	0.41	1.47	0.41	3.11	-1.22	4.94E-07	0.086	0.29
66	3.33	93.33	0.26	0.43	1.43	0.40	1.52	-0.16	3.44E-05	0.004	0.05
67	6.67	86.67	0.26	0.41	1.47	0.39	2.06	-0.15	1.96E-05	0.014	0.09
68	3.33	83.33	0.26	0.42	1.46	0.41	2.04	-0.19	1.25E-05	0.015	0.10
69	6.67	76.67	0.26	0.40	1.49	0.40	2.48	-0.19	9.70E-06	0.027	0.12
70	3.33	73.33	0.26	0.41	1.48	0.40	2.22	-0.25	7.36E-06	0.023	0.13
71	6.67	66.67	0.26	0.40	1.51	0.40	2.64	-0.25	6.08E-06	0.035	0.15
72	3.33	63.33	0.26	0.40	1.51	0.40	2.30	-0.34	4.66E-06	0.028	0.15
73	6.67	56.67	0.26	0.39	1.52	0.39	2.69	-0.35	3.97E-06	0.041	0.17
74	3.33	53.33	0.26	0.39	1.52	0.40	2.31	-0.48	2.98E-06	0.033	0.17
75	6.67	46.67	0.26	0.39	1.53	0.39	2.69	-0.49	2.59E-06	0.046	0.19
76	3.33	43.33	0.26	0.39	1.54	0.39	2.29	-0.68	1.87E-06	0.037	0.19
77	6.67	36.67	0.26	0.39	1.53	0.39	2.65	-0.69	1.65E-06	0.051	0.21
78	3.33	33.33	0.26	0.38	1.55	0.39	2.24	-0.98	1.14E-06	0.041	0.22
79	6.67	26.67	0.26	0.39	1.54	0.39	2.58	-0.96	1.01E-06	0.054	0.24
80	3.33	23.33	0.26	0.38	1.55	0.38	2.18	-1.40	6.70E-07	0.044	0.26
81	6.67	16.67	0.26	0.39	1.53	0.39	2.49	-1.34	5.99E-07	0.058	0.27
82	3.33	13.33	0.26	0.38	1.55	0.38	2.10	-1.99	3.78E-07	0.048	0.30
83	6.67	6.67	0.26	0.39	1.53	0.39	2.39	-1.85	3.40E-07	0.061	0.30
84	3.33	3.33	0.26	0.38	1.55	0.38	2.01	-2.80	2.05E-07	0.052	0.35
85	53.33	43.33	0.46	0.46	1.31	0.47	5.16	-0.27	2.12E-05	0.136	0.29

86	56.67	36.67	0.46	0.48	1.26	0.50	5.67	-0.38	1.43E-05	0.172	0.34
87	53.33	33.33	0.46	0.48	1.26	0.50	6.49	-0.35	1.00E-05	0.196	0.35
88	56.67	26.67	0.46	0.50	1.20	0.52	6.30	-0.51	8.96E-06	0.212	0.39
89	53.33	23.33	0.46	0.50	1.21	0.52	6.60	-0.48	7.52E-06	0.218	0.39
90	56.67	16.67	0.46	0.52	1.15	0.55	6.19	-0.70	6.99E-06	0.229	0.42
91	53.33	13.33	0.46	0.52	1.16	0.54	6.34	-0.64	6.00E-06	0.228	0.42
92	56.67	6.67	0.46	0.54	1.10	0.57	5.79	-0.94	5.61E-06	0.235	0.45
93	53.33	3.33	0.46	0.54	1.11	0.56	5.88	-0.85	4.74E-06	0.232	0.44
94	43.33	53.33	0.46	0.43	1.42	0.43	5.19	-0.15	2.15E-05	0.112	0.23
95	46.67	46.67	0.46	0.45	1.37	0.45	6.03	-0.19	1.44E-05	0.149	0.28
96	43.33	43.33	0.46	0.45	1.37	0.46	6.64	-0.20	9.93E-06	0.167	0.30
97	46.67	36.67	0.46	0.46	1.32	0.48	6.84	-0.25	8.88E-06	0.187	0.33
98	43.33	33.33	0.46	0.46	1.33	0.48	6.91	-0.26	7.31E-06	0.189	0.33
99	46.67	26.67	0.46	0.48	1.27	0.50	6.90	-0.34	6.82E-06	0.205	0.36
100	43.33	23.33	0.46	0.48	1.28	0.49	6.79	-0.35	5.73E-06	0.201	0.35
101	46.67	16.67	0.46	0.50	1.23	0.51	6.66	-0.45	5.39E-06	0.214	0.38
102	43.33	13.33	0.46	0.49	1.24	0.51	6.50	-0.45	4.45E-06	0.208	0.37
103	46.67	6.67	0.46	0.51	1.18	0.53	6.28	-0.59	4.18E-06	0.219	0.40
104	43.33	3.33	0.46	0.51	1.19	0.52	6.11	-0.58	3.35E-06	0.210	0.39
105	33.33	63.33	0.46	0.40	1.49	0.40	4.57	-0.11	2.22E-05	0.081	0.19
106	36.67	56.67	0.46	0.42	1.45	0.42	5.56	-0.13	1.46E-05	0.117	0.23
107	33.33	53.33	0.46	0.42	1.45	0.42	5.93	-0.14	9.90E-06	0.130	0.25
108	36.67	46.67	0.46	0.43	1.42	0.44	6.41	-0.17	8.72E-06	0.152	0.28
109	33.33	43.33	0.46	0.43	1.42	0.44	6.26	-0.19	7.05E-06	0.151	0.28
110	36.67	36.67	0.46	0.44	1.38	0.46	6.57	-0.23	6.52E-06	0.169	0.30
111	33.33	33.33	0.46	0.44	1.38	0.45	6.25	-0.25	5.36E-06	0.163	0.30
112	36.67	26.67	0.46	0.46	1.34	0.47	6.47	-0.30	5.02E-06	0.179	0.32
113	33.33	23.33	0.46	0.45	1.35	0.47	6.09	-0.33	4.06E-06	0.170	0.32
114	36.67	16.67	0.46	0.47	1.30	0.48	6.23	-0.39	3.81E-06	0.185	0.34
115	33.33	13.33	0.46	0.47	1.31	0.48	5.84	-0.43	2.98E-06	0.174	0.33
116	36.67	6.67	0.46	0.48	1.26	0.50	5.92	-0.49	2.79E-06	0.188	0.36
117	33.33	3.33	0.46	0.48	1.27	0.49	5.54	-0.54	2.10E-06	0.176	0.35
118	23.33	73.33	0.46	0.39	1.51	0.38	3.54	-0.10	2.42E-05	0.048	0.14
119	26.67	66.67	0.46	0.40	1.50	0.39	4.52	-0.11	1.53E-05	0.080	0.19
120	23.33	63.33	0.46	0.40	1.50	0.40	4.66	-0.13	1.02E-05	0.089	0.20
121	26.67	56.67	0.46	0.41	1.48	0.41	5.28	-0.15	8.74E-06	0.111	0.23
122	23.33	53.33	0.46	0.41	1.47	0.41	4.99	-0.18	6.94E-06	0.107	0.23
123	26.67	46.67	0.46	0.42	1.45	0.42	5.49	-0.20	6.26E-06	0.126	0.25
124	23.33	43.33	0.46	0.42	1.45	0.42	5.05	-0.24	5.05E-06	0.118	0.25
125	26.67	36.67	0.46	0.43	1.42	0.44	5.48	-0.26	4.65E-06	0.136	0.27
126	23.33	33.33	0.46	0.42	1.43	0.43	4.99	-0.31	3.67E-06	0.125	0.27
127	26.67	26.67	0.46	0.44	1.40	0.44	5.35	-0.34	3.41E-06	0.142	0.29
128	23.33	23.33	0.46	0.43	1.40	0.44	4.84	-0.41	2.61E-06	0.129	0.28
129	26.67	16.67	0.46	0.45	1.37	0.45	5.16	-0.44	2.42E-06	0.146	0.31
130	23.33	13.33	0.46	0.44	1.38	0.45	4.66	-0.52	1.78E-06	0.132	0.30

131	26.67	6.67	0.46	0.46	1.33	0.46	4.93	-0.55	1.65E-06	0.148	0.32
132	23.33	3.33	0.46	0.45	1.35	0.45	4.44	-0.66	1.16E-06	0.133	0.31
133	13.33	83.33	0.46	0.40	1.49	0.38	2.45	-0.12	2.85E-05	0.020	0.10
134	16.67	76.67	0.46	0.40	1.50	0.39	3.25	-0.12	1.71E-05	0.042	0.14
135	13.33	73.33	0.46	0.40	1.49	0.40	3.27	-0.15	1.13E-05	0.047	0.15
136	16.67	66.67	0.46	0.40	1.50	0.40	3.86	-0.15	9.23E-06	0.067	0.18
137	13.33	63.33	0.46	0.40	1.49	0.40	3.55	-0.19	7.19E-06	0.062	0.18
138	16.67	56.67	0.46	0.40	1.49	0.41	4.07	-0.20	6.25E-06	0.080	0.20
139	13.33	53.33	0.46	0.40	1.49	0.41	3.64	-0.26	4.94E-06	0.071	0.20
140	16.67	46.67	0.46	0.41	1.48	0.41	4.11	-0.28	4.40E-06	0.089	0.22
141	13.33	43.33	0.46	0.41	1.48	0.41	3.63	-0.35	3.40E-06	0.077	0.22
142	16.67	36.67	0.46	0.41	1.46	0.42	4.06	-0.37	3.08E-06	0.094	0.24
143	13.33	33.33	0.46	0.41	1.47	0.41	3.56	-0.48	2.30E-06	0.082	0.24
144	16.67	26.67	0.46	0.42	1.45	0.42	3.96	-0.49	2.09E-06	0.099	0.26
145	13.33	23.33	0.46	0.41	1.46	0.42	3.46	-0.63	1.50E-06	0.085	0.26
146	16.67	16.67	0.46	0.42	1.43	0.43	3.82	-0.64	1.37E-06	0.101	0.28
147	13.33	13.33	0.46	0.42	1.44	0.42	3.33	-0.83	9.38E-07	0.087	0.27
148	16.67	6.67	0.46	0.43	1.41	0.43	3.66	-0.82	8.58E-07	0.103	0.29
149	13.33	3.33	0.46	0.43	1.43	0.42	3.19	-1.08	5.62E-07	0.089	0.29
150	3.33	93.33	0.46	0.43	1.40	0.41	1.58	-0.16	3.68E-05	0.005	0.06
151	6.67	86.67	0.46	0.42	1.45	0.40	2.14	-0.15	2.10E-05	0.016	0.09
152	3.33	83.33	0.46	0.42	1.43	0.41	2.12	-0.19	1.35E-05	0.018	0.11
153	6.67	76.67	0.46	0.41	1.46	0.40	2.56	-0.19	1.05E-05	0.030	0.13
154	3.33	73.33	0.46	0.42	1.45	0.41	2.31	-0.25	8.02E-06	0.026	0.13
155	6.67	66.67	0.46	0.41	1.47	0.41	2.72	-0.25	6.64E-06	0.038	0.16
156	3.33	63.33	0.46	0.41	1.47	0.41	2.38	-0.33	5.13E-06	0.031	0.16
157	6.67	56.67	0.46	0.41	1.48	0.40	2.77	-0.34	4.38E-06	0.045	0.18
158	3.33	53.33	0.46	0.40	1.48	0.41	2.38	-0.46	3.31E-06	0.036	0.18
159	6.67	46.67	0.46	0.40	1.49	0.40	2.76	-0.46	2.88E-06	0.049	0.20
160	3.33	43.33	0.46	0.40	1.50	0.40	2.36	-0.63	2.10E-06	0.039	0.20
161	6.67	36.67	0.46	0.40	1.49	0.40	2.71	-0.63	1.85E-06	0.053	0.22
162	3.33	33.33	0.46	0.40	1.50	0.40	2.30	-0.88	1.29E-06	0.043	0.22
163	6.67	26.67	0.46	0.40	1.49	0.40	2.64	-0.87	1.15E-06	0.057	0.24
164	3.33	23.33	0.46	0.40	1.51	0.40	2.23	-1.23	7.65E-07	0.046	0.25
165	6.67	16.67	0.46	0.40	1.49	0.40	2.55	-1.18	6.85E-07	0.059	0.27
166	3.33	13.33	0.46	0.40	1.50	0.40	2.15	-1.69	4.36E-07	0.049	0.29
167	6.67	6.67	0.46	0.41	1.48	0.40	2.44	-1.58	3.91E-07	0.062	0.29
168	3.33	3.33	0.46	0.40	1.50	0.39	2.06	-2.31	2.38E-07	0.051	0.33
169	53.33	43.33	1.12	0.46	1.30	0.46	5.79	-0.25	1.81E-05	0.153	0.30
170	56.67	36.67	1.12	0.48	1.25	0.49	6.44	-0.34	1.20E-05	0.190	0.34
171	53.33	33.33	1.12	0.48	1.25	0.50	7.27	-0.32	8.79E-06	0.214	0.36
172	56.67	26.67	1.12	0.50	1.19	0.52	7.14	-0.45	7.78E-06	0.230	0.39
173	53.33	23.33	1.12	0.50	1.19	0.52	7.38	-0.43	6.78E-06	0.236	0.40
174	56.67	16.67	1.12	0.52	1.14	0.54	6.99	-0.61	6.24E-06	0.247	0.43

175	53.33	13.33	1.12	0.52	1.13	0.54	7.05	-0.57	5.56E-06	0.247	0.42
176	56.67	6.67	1.12	0.54	1.08	0.57	6.51	-0.81	5.14E-06	0.253	0.46
177	53.33	3.33	1.12	0.55	1.07	0.56	6.50	-0.75	4.50E-06	0.249	0.45
178	43.33	53.33	1.12	0.43	1.38	0.43	5.66	-0.15	1.95E-05	0.127	0.25
179	46.67	46.67	1.12	0.45	1.34	0.45	6.63	-0.19	1.29E-05	0.165	0.29
180	43.33	43.33	1.12	0.45	1.33	0.46	7.25	-0.19	9.26E-06	0.184	0.31
181	46.67	36.67	1.12	0.47	1.29	0.48	7.52	-0.24	8.19E-06	0.205	0.34
182	43.33	33.33	1.12	0.47	1.28	0.49	7.53	-0.25	6.99E-06	0.207	0.34
183	46.67	26.67	1.12	0.49	1.24	0.50	7.57	-0.32	6.45E-06	0.223	0.37
184	43.33	23.33	1.12	0.49	1.23	0.50	7.40	-0.33	5.61E-06	0.220	0.37
185	46.67	16.67	1.12	0.51	1.18	0.52	7.29	-0.42	5.23E-06	0.233	0.39
186	43.33	13.33	1.12	0.51	1.18	0.52	7.05	-0.42	4.47E-06	0.226	0.39
187	46.67	6.67	1.12	0.53	1.13	0.54	6.83	-0.54	4.15E-06	0.237	0.41
188	43.33	3.33	1.12	0.53	1.13	0.54	6.59	-0.53	3.44E-06	0.228	0.41
189	33.33	63.33	1.12	0.42	1.43	0.41	4.90	-0.12	2.13E-05	0.094	0.20
190	36.67	56.67	1.12	0.43	1.41	0.43	5.99	-0.13	1.39E-05	0.132	0.25
191	33.33	53.33	1.12	0.43	1.39	0.44	6.37	-0.15	9.76E-06	0.146	0.27
192	36.67	46.67	1.12	0.44	1.36	0.45	6.92	-0.17	8.52E-06	0.169	0.29
193	33.33	43.33	1.12	0.45	1.35	0.46	6.73	-0.19	7.12E-06	0.169	0.30
194	36.67	36.67	1.12	0.46	1.32	0.47	7.10	-0.22	6.52E-06	0.187	0.32
195	33.33	33.33	1.12	0.46	1.31	0.47	6.73	-0.25	5.54E-06	0.181	0.32
196	36.67	26.67	1.12	0.47	1.27	0.49	6.99	-0.29	5.15E-06	0.198	0.34
197	33.33	23.33	1.12	0.48	1.27	0.49	6.55	-0.31	4.29E-06	0.189	0.34
198	36.67	16.67	1.12	0.49	1.23	0.50	6.72	-0.36	3.99E-06	0.204	0.36
199	33.33	13.33	1.12	0.49	1.23	0.50	6.27	-0.39	3.22E-06	0.193	0.35
200	36.67	6.67	1.12	0.51	1.18	0.52	6.35	-0.45	2.99E-06	0.206	0.38
201	33.33	3.33	1.12	0.51	1.18	0.51	5.93	-0.48	2.32E-06	0.194	0.37
202	23.33	73.33	1.12	0.41	1.45	0.40	3.78	-0.11	2.42E-05	0.058	0.16
203	26.67	66.67	1.12	0.42	1.44	0.41	4.82	-0.12	1.53E-05	0.092	0.20
204	23.33	63.33	1.12	0.42	1.42	0.42	4.99	-0.14	1.05E-05	0.103	0.22
205	26.67	56.67	1.12	0.43	1.40	0.43	5.65	-0.15	8.97E-06	0.126	0.25
206	23.33	53.33	1.12	0.43	1.39	0.44	5.35	-0.18	7.34E-06	0.123	0.25
207	26.67	46.67	1.12	0.44	1.37	0.45	5.89	-0.19	6.59E-06	0.143	0.27
208	23.33	43.33	1.12	0.44	1.36	0.45	5.42	-0.23	5.48E-06	0.135	0.27
209	26.67	36.67	1.12	0.45	1.34	0.46	5.88	-0.25	5.01E-06	0.154	0.29
210	23.33	33.33	1.12	0.45	1.33	0.46	5.36	-0.29	4.08E-06	0.142	0.29
211	26.67	26.67	1.12	0.46	1.30	0.47	5.75	-0.31	3.76E-06	0.160	0.31
212	23.33	23.33	1.12	0.46	1.30	0.47	5.21	-0.37	2.96E-06	0.147	0.31
213	26.67	16.67	1.12	0.48	1.27	0.48	5.55	-0.39	2.73E-06	0.164	0.33
214	23.33	13.33	1.12	0.48	1.27	0.48	5.01	-0.45	2.06E-06	0.149	0.32
215	26.67	6.67	1.12	0.49	1.23	0.49	5.29	-0.48	1.89E-06	0.165	0.34
216	23.33	3.33	1.12	0.49	1.23	0.49	4.78	-0.55	1.37E-06	0.150	0.33
217	13.33	83.33	1.12	0.42	1.41	0.40	2.67	-0.12	2.94E-05	0.028	0.12
218	16.67	76.67	1.12	0.42	1.43	0.41	3.51	-0.12	1.77E-05	0.053	0.16
219	13.33	73.33	1.12	0.43	1.41	0.42	3.56	-0.15	1.20E-05	0.060	0.18

220	16.67	66.67	1.12	0.43	1.41	0.42	4.16	-0.15	9.81E-06	0.081	0.20
221	13.33	63.33	1.12	0.43	1.39	0.43	3.85	-0.19	7.86E-06	0.076	0.20
222	16.67	56.67	1.12	0.43	1.39	0.43	4.39	-0.20	6.83E-06	0.095	0.23
223	13.33	53.33	1.12	0.44	1.38	0.44	3.94	-0.25	5.54E-06	0.086	0.23
224	16.67	46.67	1.12	0.44	1.37	0.44	4.43	-0.26	4.94E-06	0.105	0.25
225	13.33	43.33	1.12	0.44	1.37	0.44	3.93	-0.32	3.92E-06	0.092	0.24
226	16.67	36.67	1.12	0.45	1.35	0.45	4.38	-0.33	3.54E-06	0.111	0.26
227	13.33	33.33	1.12	0.45	1.35	0.45	3.86	-0.41	2.71E-06	0.096	0.26
228	16.67	26.67	1.12	0.45	1.33	0.45	4.28	-0.42	2.46E-06	0.114	0.28
229	13.33	23.33	1.12	0.45	1.33	0.45	3.75	-0.52	1.81E-06	0.099	0.27
230	16.67	16.67	1.12	0.46	1.30	0.46	4.13	-0.52	1.65E-06	0.117	0.29
231	13.33	13.33	1.12	0.46	1.31	0.46	3.62	-0.64	1.16E-06	0.101	0.29
232	16.67	6.67	1.12	0.47	1.28	0.47	3.97	-0.63	1.05E-06	0.117	0.31
233	13.33	3.33	1.12	0.47	1.28	0.46	3.47	-0.78	7.11E-07	0.101	0.30
234	3.33	93.33	1.12	0.46	1.32	0.43	1.78	-0.18	3.82E-05	0.010	0.08
235	6.67	86.67	1.12	0.44	1.36	0.42	2.38	-0.16	2.20E-05	0.024	0.12
236	3.33	83.33	1.12	0.45	1.33	0.44	2.38	-0.21	1.45E-05	0.027	0.14
237	6.67	76.67	1.12	0.44	1.37	0.43	2.84	-0.19	1.14E-05	0.041	0.16
238	3.33	73.33	1.12	0.45	1.35	0.44	2.58	-0.25	8.87E-06	0.037	0.16
239	6.67	66.67	1.12	0.44	1.37	0.44	3.00	-0.25	7.40E-06	0.051	0.18
240	3.33	63.33	1.12	0.45	1.35	0.44	2.65	-0.32	5.85E-06	0.043	0.18
241	6.67	56.67	1.12	0.44	1.37	0.44	3.05	-0.32	5.03E-06	0.058	0.20
242	3.33	53.33	1.12	0.44	1.36	0.44	2.65	-0.41	3.89E-06	0.047	0.20
243	6.67	46.67	1.12	0.44	1.37	0.44	3.04	-0.41	3.40E-06	0.062	0.22
244	3.33	43.33	1.12	0.44	1.36	0.44	2.61	-0.53	2.54E-06	0.050	0.22
245	6.67	36.67	1.12	0.44	1.36	0.44	2.98	-0.52	2.25E-06	0.065	0.24
246	3.33	33.33	1.12	0.44	1.36	0.44	2.54	-0.68	1.61E-06	0.053	0.24
247	6.67	26.67	1.12	0.45	1.35	0.44	2.90	-0.67	1.43E-06	0.068	0.25
248	3.33	23.33	1.12	0.45	1.35	0.44	2.46	-0.88	9.81E-07	0.054	0.26
249	6.67	16.67	1.12	0.45	1.34	0.44	2.80	-0.84	8.76E-07	0.069	0.27
250	3.33	13.33	1.12	0.45	1.34	0.44	2.38	-1.11	5.74E-07	0.056	0.28
251	6.67	6.67	1.12	0.46	1.32	0.45	2.69	-1.04	5.13E-07	0.070	0.29
252	3.33	3.33	1.12	0.45	1.33	0.44	2.28	-1.38	3.21E-07	0.056	0.30
253	n/a	n/a	≥8.72	n/a	n/a	0.80	3.41	-1.76	7.86E-07	0.216	0.66

Table 3: Highly refined soil classes and soil hydraulic properties where for the 0-30cm top soil layer: Cl is the percentage clay ; Sa is the percentage sand; OC is the organic carbon content; $\boldsymbol{\Theta_s^*}$ is the first approximation of soil moisture content at saturation that was used in pedotransfer functions to derive hydraulic properties; ρ_b is the soil bulk density; $\boldsymbol{\Theta_s}$ is the soil moisture content at saturation; b is a parameter describing the shape of the water retention curve; $\boldsymbol{\Psi_s}$ is the matric potential at saturation; $\mathbf{K_s}$ is the hydraulic conductivity at saturation; wp is the wilting point; fc is the field capacity (adapted from De Lannoy et al., 2014).

5. SEASONALLY-VARYING VEGETATION DATA

5.1 Data generation and processing chain

The Second Global Soil Wetness Project (GSWP-2) provided monthly Leaf Area Index (LAI) and Greenness Fraction (GrnFrac) data on a 1°×1° grid for the period 1982-1998. A monthly climatology of GrnFrac was computed from these data by temporally averaging over the 17-year period (by month) on the 1°×1° grid and then spatially interpolating the averages onto 30-arcsec pixels. The interpolated GrnFrac data were aggregated over the pixels of each land element to derive a monthly GrnFrac climatology for that land element.

Global, 10-day averaged LAI data on a 40320×20160 grid for the period 1999-2011 are available from GEOLAND2 (Baret et al., 2012 and Camacho et el. 2013). In addition, 8-day composites of MOD15A2 v005 MODIS LAI data (MODIS, 2008) are available at 30-arcsec (43200×21600) for the period 2000-2013. Preprocessing of the two datasets showed that each had potential flaws, with GEOLAND2 showing questionable seasonal cycles in Siberia, and MODIS showing questionable values over the rain forests. We thus decided to produce a merged LAI data product for GEOS-5 to avoid these potential deficiencies.

The first step in generating the merged product was computing a 10-day climatology of GEOLAND LAI at each GEOLAND2 pixel from the 13 years of GEOLAND2 data and then spatially aggregating the pixel-based climatologies to surface elements. The next step was computing the corresponding 8-day MODIS-based LAI climatology for each surface element from the 14-years of MODIS data. To do this, we used MODIS auxiliary data on surface type to fill in LAI values at certain land pixels as follows: barren, rock, and desert surface types were given LAI values of 0.01, urban-built areas were given values of 0.5; and marshland areas were given values obtained from nearest neighbor pixels. The filled-in MODIS data had to be projected from a sinusoidal grid to a regular latitude/longitude grid prior to the calculation of the pixel-based 8-day climatologies and the subsequent spatial aggregation of the pixel climatologies to surface element climatologies.

Note that in high latitudes, both MODIS and GEOLAND2 data are not available over large areal swaths. To address this, we constructed, at every time slice (8 days for MODIS and 10 days for GEOLAND2), a 1°×1° global gridded LAI dataset by spatially aggregating the finer resolution LAI climatological data. Missing LAI values in the finer resolution datasets were filled with the value for the 'nearest neighbor' on the 1°×1° global grid.

To merge the GEOLAND2 and MODIS data into a single product of 8-day LAI climatologies, the 10-day GEOLAND2 climatological seasonal cycle at each element was first time-interpolated to the 8-day cycle used by MODIS. MODIS LAI data were then selected for all surface elements except those in South America, Africa and Australia, which took their values from the GEOLAND2 LAI dataset. Figure 9 shows global maps of climatological mean monthly of LAI for the merged LAI data.

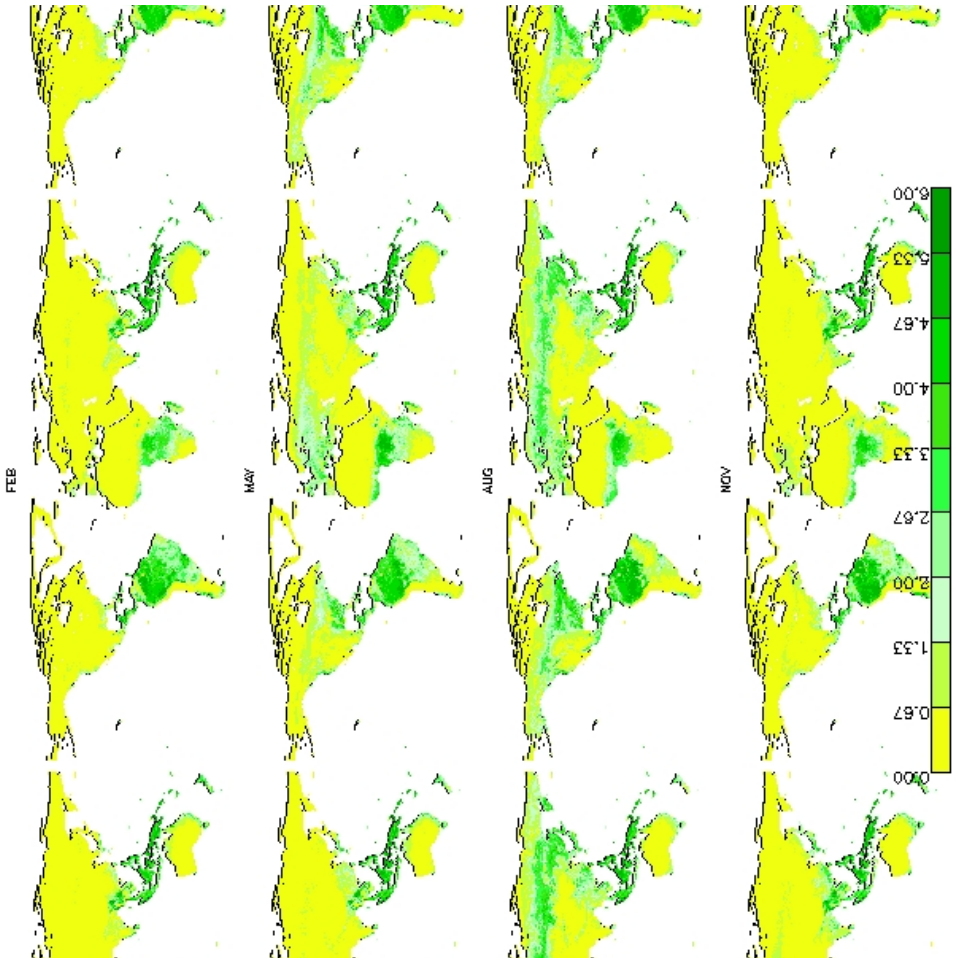

5.2 Data files and movies

5.2.1 Greenness Fraction [-]

```
file name  : green.dat (or ../green_clim*.data)
file format: fortran binaries, little_endian
The read statement should be MAPL_ReadForcing compatible.
     Each data record is preceded by a header containing
     the start and end times of the period over which the
     data have been averaged. Corresponding start dates for
     climatological data records are: 1201 0101 0201 0301
     0401 0501 0601 0701 0801 0901 1001 1101 1201 0101
     (MMDD: where MM is month and DD is day of month)

Reading data: Loop over the next two lines until the last
     data record is read.
read(10) Year_Begin, Month_Begin, Day_Begin, Hour_Begin,
     Minute_Begin, Secs_Begin, Year_End, Month_End,
     Day_End, Hour_End, Minute_End, Secs_End (Float
     Numbers)
```

Figure 9: Mean monthly Leaf Area Index (LAI) for the merged data.

```
read(10) (data(n),n=1,NTILES)
```

5.2.2 Leaf Area Index (LAI) [m^2/m^2]

```
file name  : lai.dat (or ../lai_clim*.data)
file format: fortran binaries, little_endian
The read statement should be MAPL_ReadForcing compatible.
     Each data record is preceded by a header containing
     the start and end times of the period over which the
     data have been averaged. Corresponding start dates for
     climatological data records are: 1227 0101 0109 0117
     0125 0202 0210 0218 0226 0306 0314 0322 0330 0407 0415
     0423 0501 0509 0517 0525 0602 0610 0618 0626 0704 0712
     0720 0728 0805 0813 0821 0829 0906 0914 0922 0930 1008
     1016 1024 1101 1109 1117 1125 1203 1211 1219 1227 0101
     (MMDD: where MM is month and DD is day of month)
Reading data: Loop over the next two lines until the last
     data record is read.
read(10) Year_Begin, Month_Begin, Day_Begin, Hour_Begin,
     Minute_Begin, Secs_Begin, Year_End, Month_End,
     Day_End, Hour_End, Minute_End, Secs_End (Float
     Numbers)
read(10) (data(n),n=1,NTILES)
```

6. SURFACE ALBEDO DATA

6.1 Data generation and processing chain

The Catchment Land Surface Model (CLSM) computes, at each model time step, the following quantities: (1) visible (0.3-0.7μm) direct albedo (black sky), (2) near-infrared (0.7-5.0μm) direct albedo, (3) visible (0.3-0.7μm) diffuse albedo (white sky), and (4) near-infrared (0.7-5.0μm) diffuse albedo. Initial diurnally-varying values are first computed using an albedo scheme (Koster and Suarez 1991) based on the two-stream approximation utilized by SiB (Sellers et al. 1986). These values are then scaled so that their 8-day averages agree with a MODIS-based albedo climatology.

To compute the scaling factors, 30-arcsec 8-day composites of MODIS (MCD43GF, 2014 and Gao et al., 2014) diffuse visible (VISDF) and diffuse near-infrared data (NIRDF) from the period 2001-2011 were temporally averaged into an 8-day climatology. These 30-arcsec climatological values were then spatially averaged over a given land surface element's pixels to produce an 8-day climatology for the land element as a whole.

Meanwhile, the SiB-based albedo scheme was run at a daily time step over a 1-year period using the vegetation types, greenness fractions, and leaf area indices established for GEOS-5 for a given distribution of land elements, as described in sections 3.2.1, 5.2.1, and 5.2.2 above. Averaging the visible diffuse and near-infrared diffuse albedos generated by the scheme over 8-day periods produced, in effect, an 8-day 'climatology' of this particular scheme's diffuse albedos. The ratio of the MODIS-based 8-day diffuse visible albedo to the SiB-based diffuse visible albedo at a given surface element serves as the 8-day 'scaling factor' for that element. During a full simulation, the time-step values of both the visible direct and visible diffuse albedos computed with the SiB-based scheme are multiplied by the diffuse-based scale factor (for the given element and given 8-day period) prior to being applied to the incoming radiation values. The same approach is used to compute the scale factors for the near-infrared albedos.

6.2 Data files and movies

6.2.1 MODIS Albedo Climatology [Diffuse, Visible (0.3-0.7μm) and Near-Infrared (0.7-5.0μm)]

Note: CLSM does not use MODIS albedo data explicitly.

```
file names : AlbMap.WS.8-day.tile.0.3_0.7.dat/AlbMap.WS.8-
     day.tile.0.7_5.0.dat

file format: fortran binaries, little_endian

The read statement should be MAPL_ReadForcing compatible.
     Each data record is preceded by a header containing
     start and end times of the period over which the data
     have been averaged. Corresponding start dates for
     climatological data records are: 1227 0101 0109 0117
     0125 0202 0210 0218 0226 0306 0314 0322 0330 0407 0415
     0423 0501 0509 0517 0525 0602 0610 0618 0626 0704 0712
     0720 0728 0805 0813 0821 0829 0906 0914 0922 0930 1008
     1016 1024 1101 1109 1117 1125 1203 1211 1219 1227 0101
     (MMDD: where MM is month and DD is day of year)
Reading data: Loop over the next two lines until the last
     data record is read.
read(10) Year_Begin, Month_Begin, Day_Begin, Hour_Begin,
     Minute_Begin, Secs_Begin, Year_End, Month_End,
     Day_End, Hour_End, Minute_End, Secs_End (Float
     Numbers)
read(10) (data(n),n=1,NTILES)
```

6.2.2 MODIS Scale Parameters [Diffused, Visible (0.3_0.7) and Near-Infrared (0.7_5.0)]

```
file names : visdf.dat/nirdf.dat (or ../visdf*dat and
     ../nirdf*dat)
file format: fortran binaries, little_endian
The read statement should be MAPL_ReadForcing compatible.
     Each data record is preceded by a header containing
     start and end times of the period over which the data
     have been averaged. Corresponding start dates for
     climatological data records are: 1227 0101 0109 0117
     0125 0202 0210 0218 0226 0306 0314 0322 0330 0407 0415
     0423 0501 0509 0517 0525 0602 0610 0618 0626 0704 0712
     0720 0728 0805 0813 0821 0829 0906 0914 0922 0930 1008
     1016 1024 1101 1109 1117 1125 1203 1211 1219 1227 0101
     (MMDD: where MM is month and DD is day of year)
Reading data: Loop over the next two lines until the last
     data record is read.
read(10) Year_Begin, Month_Begin, Day_Begin, Hour_Begin,
     Minute_Begin, Secs_Begin, Year_End, Month_End,
     Day_End, Hour_End, Minute_End, Secs_End (Float
     Numbers)
read(10) (data(n),n=1,NTILES)
```

7. CATCHMENT LAND SURFACE MODEL PARAMETERS

7.1 Data generation and processing chain

The Catchment LSM utilizes numerous preprocessed parameters, many of which describe ‘fits’ to the results of highly complex calculations. For efficiency purposes, these fits are used in place of the complex calculations themselves during simulations. The parameters derived for each surface element rely in part on the statistics of compound topographic index in "cti_stats.dat" (Section 4.2.3) and the soil hydraulic properties in "soil_param.dat" (Section 4.2.4). The user is referred to Ducharne et al. (2000) for a description of the CLSM parameter generation process and for definitions of the parameters themselves.

7.2 Data files

In the descriptions below, equation and figure numbers refer to those in Ducharne et al. (2000).

7.2.1 Time scale parameters for moisture transfer between surface excess and root zone excess prognostic variables

```
file name : tau_param.dat
do n = 1, NTILES
     read (10,'(i8,i8,4f10.7)')tile_index, pfaf_index,
     atau2, btau2, atau5, btau5
end do
where:
(1) gnu   vertical transmissivity parameter {ν in Equation
     (8)} [m-1]
(2) atau2 a_τ2 in Equation (17) for a 2cm surface layer [-]
(3) btau2 b_τ2 in Equation (17) for a 2cm surface layer [-]
(4) atau5 a_τ2 in Equation (17) for a 5cm surface layer [-]
(5) btau5 a_τ2 in Equation (17) for a 5cm surface layer [-]
```

6.2.2 Time scale parameters for moisture transfer between root zone excess and catchment deficit prognostic variables

```
file name : ts.dat
do n = 1, NTILES
     read(10,'(i8,i8,f5.2,4(2x,e13.7))')tile_index,
     pfaf_index, gnu, tsa1, tsa2, tsb1, tsb2
end do

where:
(1) gnu   vertical transmissivity parameter {ν in Equation
     (8)} [m-1]
(2) tsa1  a_τ1 in Equation (16) for positive root zone excess
     (Ducharne et al., 2000: Figure 6) [-]
(3) tsa2  a_τ1 in Equation (16) for negative root zone excess
     (Ducharne et al., 2000: Figure 6) [-]
(4) tsb1  b_τ1 in Equation (16) for positive root zone excess
     (Ducharne et al., 2000: Figure 6) [-]
(5) tsb2  b_τ1in Equation (16) for negative root zone excess
     (Ducharne et al., 2000: Figure 6) [-]
```

7.2.3 Baseflow parameters

```
file name : bf.dat
```

```
do n = 1, NTILES
     read(10,'(i8,i8,f5.2,3(2x,e13.7))')tile_index,
     pfaf_index, gnu, bf1, bf2, bf3
end do

where:
(1) gnu   vertical transmissivity parameter {ν in Equation
     (8)} [m-1]
(2) bf1   A in Equation (9)   [kg m-4]
(3) bf2   B in Equation (9)   [m]
(4) bf3   XBAR in Equation (8) (same as cti_mean in Section
     4.2.2) [log(m)]
```

7.2.4 Area fractioning parameters

```
file name : ar.new
do n = 1, NTILES
read(10,'(i8,i8,f5.2,11(2x,e13.7))')tile_index, pfaf_index,
     gnu, ars1, ars2, ars3, ara1,ara2, ara3, ara4, arw1,
     arw2, arw3, arw4
end do

where:
(1) gnu   vertical transmissivity parameter {ν in Equation
     (8)} [m-1]
(2) ars1  A in Equation (12) for A_sat [m+2 kg-1]
(3) ars2  B in Equation (12) for A_sat [m+2 kg-1]
(4) ars3  C in Equation (12) for A_sat [m+4 kg-2]
(5) ara1  A in Equation (14) of segment1 if skewness < 0.25
     [m+2 kg-1] | (else ara1 = ara3)
(6) ara2  B in Equation (14) of segment1 if skewness < 0.25
     [-]        | (else ara2 = ara4)
(7) ara3  A in Equation (14) of segment2 if skewness < 0.25
     [m+2 kg-1]
(8) ara4  B in Equation (14) of segment2 if skewness < 0.25
     [-]
(9) arw1  A in Equation (12) for Θ0 [m+2 kg-1]
(10)arw2  B in Equation (12) for Θ0 [m+2 kg-1]
(11)arw3  C in Equation (12) for Θ0 [m+4 kg-2]
(12)arw4  Y∞ in Equation (12) for Θ0 [-]
```

8. GLOBAL RUNOFF ROUTING MODEL DATA

8.1 Data generation and processing chain

The Pfafstetter codification (Verdin and Verdin, 1999) assigns a unique multi-digit integer to a given hydrologic catchment within a river basin. The multi-digit integer, or Pfafstetter code, contains information about connectivity of the catchment with upstream and downstream catchments; considering all of the catchments' codes together allows the construction of a catchment network within the basin. Verdin (2013) provided global raster arrays of global Level 12 Pfafstetter codes at 1-arcmin resolution along with information on mean elevation. These data sets were used to build the global river channel network slated for use with GEOS-5 (see, e.g,Figure 10).

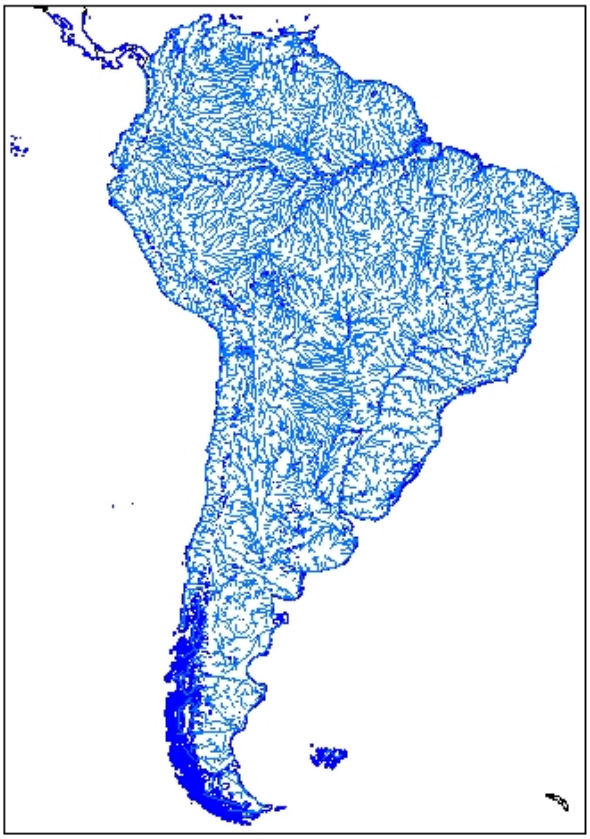

Figure 10: Illustration of river channel network in South America.

The steps used to generate the river network are as follows. Each catchment (referred to in this discussion as CatchX) has typically zero or two upstream catchments (although some catchments may have one or more than two, as discussed below) but only one downstream catchment (or only one sink, as an ocean or a lake). The Pfafstetter code helps locate the downstream catchment. Once it is identified, CatchX automatically becomes one of the upstream catchments for the downstream catchment. During the Pfafstetter codification process, sometimes islands can be incorrectly linked across the ocean. Sinks also often get incorrectly linked with catchments geographically far apart. Thus, a land-water mask at 1 arc-minute resolution was created using the 10 arc-second mask (Section 2) created to help identify islands and coastal catchments. Islands, coastal catchments and sinks were given due attention to ensure that they don't get linked up incorrectly. The 1 arc-minute elevation data were used to determine the lowest point (outlet) of each catchment.

Once the upstream and downstream catchments for CatchX are identified, the next step is to find the latitudinal and longitudinal coordinates of its upstream and downstream confluences. This is complicated by the fact that the codification at 1-arcmin is imperfect – in a perfect system, a catchment would only have zero or two upstream catchments, but because of the discretization to 1-arcmin and the associated loss of higher resolution information, a catchment might end up having (according to the discretized codification) one or possibly more than two upstream catchments. To determine the locations of the upstream confluences, we must therefore consider four possible cases:

Case 1: CatchX has no upstream catchments. In this case, the centroid of CatchX is used as the location of the upstream confluence, for purposes of computing river length and elevation difference.
Case 2: There is only one upstream catchment. The nearest 1-arcmin CatchX pixel to the centroid of the upstream catchment is assumed to be the upstream confluence.
Case 3: Exactly 2 upstream catchments are present. The meeting point of CatchX and the two upstream catchments is determined and assigned to be the location of the upstream confluence.
Case 4: There are more than 2 upstream catchments. For each 1-arcmin pixel within CatchX, the sum of the distances between the pixel and the centroids of each upstream catchment is computed. The pixel with the minimum sum-of-distances is assumed to be located at the upstream confluence.

To determine the location of the downstream confluence, only two cases need to be considered:

Case 1: There is a downstream catchment. The location of the downstream confluence of CatchX is taken to be the same as that of the upstream confluence for that downstream catchment.
Case 2: There is no downstream catchment. A 1-arcmin CatchX pixel located next to a water pixel is assumed to be the location of the downstream confluence.

8.2 Data files

8.2.1 Pfafstetter watershed connectivity, channel information

```
file name: /discover/nobackup/smahanam/l_data/
     LandBCs_files_for_mkCatchParam/SRTM-TopoData/
     Pfafcatch-routing.dat
read (10,*) NPfafs

do n = 1, NPfafs
read(10,'(i8,i15,4(1x,f9.4),1x,e10.3,3(1x,e9.3),I8,6(1x,f9.
     4))') pfaf_index, pfaf_code, min_lon, max_lon,
     min_lat, max_lat, mean_elevation, cat_area,length,
     ElevDiff, dnst_pfaf_index, DN_long, DN_lat, UP_lon,
     UP_lat, mouth_lon, mouth_lat
end do

pfaf_index     catchment index (1-291284) after sorting
     Pfafstetter codes in ascending order [-]
pfaf_code      Pfafstetter code of the hydrologic catchment
     [-]
min_lon        Longitude of westernmost edge of the
     catchment [degree]
max_lon        Longitude of easternmost edge of the
     catchment [degree]
min_lat        Latitude of southernmost edge of the
     catchment [degree]
max_lat        Latitude of northernmost edge of the
     catchment [degree]
mean_elevation Area-averaged elevation [m]
cat_area       catchment area [km2]
Length         Distance between upstream and downstream
               confluences [km]
ElevDiff       Elevation difference between upstream and
               downstream confluences [m]
DN_pfaf_index  catchment index of the downstream catchment
               (Note : -1 depicts a sink or lake/ocean) [-]
DN_long        longitude at the downstream confluence
               [degree]
DN_lat         latitude at the downstream confluence
               [degree]
UP_lon         longitude at the upstream confluence
               [degree]
UP_lat         latitude at the upstream confluence [degree]
mouth_lon      longitude at the river mouth [degree]
mouth_lat      latitude at the river mouth [degree]
```

8.2.2 Fractional areas to aggregate from SMAP grid cells to Pfafstetter watersheds

Because surface catchment elements for AGCM grids are derived by overlaying AGCM grids on the Pfafstetter watershed map, information in the BCRSLV-Pfafstetter.til file (Section 4.2.1) can be used to convert variables between computational surface elements and Pfafstetter watersheds. However, quasi-rectangular SMAP grid cells are completely independent of Pfafstetter watershed boundaries. The self-describing SMAP-Catch_TransferData.nc file contains the information needed to convert between SMAP grid cells and watersheds. The information includes the number of Pfafstetter watersheds contributing to the SMAP grid cell and the fractional areas of those contributing watersheds.

```
file name : SMAP-Catch_TransferData.nc


where :

NCats_in_SMAP  No. of pfaf catchments contributing to the
               SMAP cell
Pfaf_Index     Pfaf indices (1-291,284) of those
               contributing catchments
Pfaf_Area[km2] Area of the Pfaf Catchment fraction
Pfaf_Frac [-]  Fraction of Pfaf catchment contributing to
               the SMAP cell
```

REFERENCES

Arendt, A., A. Bliss, T. Bolch, J.G. Cogley, A.S. Gardner, J.-O. Hagen, R. Hock, M. Huss, G. Kaser, C. Kienholz, W.T. Pfeffer, G. Moholdt, F. Paul, V. Radić, L. Andreassen, S. Bajracharya, N. Barrand, M. Beedle, E. Berthier, R. Bhambri, I. Brown, E. Burgess, D. Burgess, F. Cawkwell, T. Chinn, L. Copland, B. Davies, H. De Angelis, E. Dolgova, K. Filbert, R. Forester, A. Fountain, H. Frey, B. Giffen, N. Glasser, S. Gurney, W. Hagg, D. Hall, U.K. Haritashya, G. Hartmann, C. Helm, S. Herreid, I. Howat, G. Kapustin, T. Khromova, M. König, J. Kohler, D. Kriegel, S. Kutuzov, I. Lavrentiev, R. LeBris, J. Lund, W. Manley, C. Mayer, E.S. Miles, X. Li, B. Menounos, A. Mercer, N. Mölg, P. Mool, G. Nosenko, A. Negrete, C. Nuth, R. Pettersson, A. Racoviteanu, R. Ranzi, P. Rastner, F. Rau, B. Raup, J. Rich, H. Rott, C. Schneider, Y. Seliverstov, M. Sharp, O. Sigurðsson, C. Stokes, R. Wheate, S. Winsvold, G. Wolken, F. Wyatt, N. Zheltyhina, (2014): Randolph Glacier Inventory – A Dataset of Global Glacier Outlines: Version 4.0. Global Land Ice Measurements from Space, Boulder Colorado, USA. Digital Media.

Baret, F., M. Weiss1, R. Lacaze, F. Camacho, H. Makhmara, P. Pacholcyzk and B. Smets (2012): GEOV1: LAI, FAPAR Essential Climate Variables and FCOVER global time

series capitalizing over existing products. Part1: Principles of development and production. Remote Sensing Environment, 137, 299-309 doi:10.1016/j.rse.2012.12.027

Camacho, F., J. Cernicharo, R. Lacaze F. Baret, M. Weiss (2013): GEOV1: LAI, FAPAR Essential Climate Variables and FCover global time series capitalizing over existing products. Part 2: Validation and inter-comparison with reference products Remote Sensing of Enviroment, 137, 310–329, doi:10.1016/j.rse.2013.02.030

De Lannoy, G. J. M., R. D. Koster, R. H. Reichle, S. P. P. Mahanama, and Q. Liu (2014): An updated treatment of soil texture and associated hydraulic properties in a global land modeling system, J. Adv. Model. Earth Syst., 06, doi:10.1002/2014MS000330.

Dirmeyer, P. and Oki, T. (2002): The Second Global Soil Wetness project (GSWP-2) Science 2 and Implementation Plan. IGPO Publication Series No. 37, 64p.

Ducharne, A., R. D. Koster, M. J. Suarez, M. Stieglitz, and P. Kumar (2000): A catchment-based approach to modeling land surface processes in a general circulation model: 2. Parameter estimation and model demonstration, J. Geophys. Res., 105(D20), 2482324838, doi:10.1029/2000JD900328.

Fretwell, P., Pritchard, H. D., Vaughan, D. G., Bamber, J. L., Barrand, N. E., Bell, R., Bianchi, C., Bingham, R. G., Blankenship, D. D., Casassa, G., Catania, G., Callens, D., Conway, H., Cook, A. J., Corr, H. F. J., Damaske, D., Damm, V., Ferraccioli, F., Forsberg, R., Fujita, S., Gim, Y., Gogineni, P., Griggs, J. A., Hindmarsh, R. C. A., Holmlund, P., Holt, J. W., Jacobel, R. W., Jenkins, A., Jokat, W., Jordan, T., King, E. C., Kohler, J., Krabill, W., Riger-Kusk, M., Langley, K. A., Leitchenkov, G., Leuschen, C., Luyendyk, B. P., Matsuoka, K., Mouginot, J., Nitsche, F. O., Nogi, Y., Nost, O. A., Popov, S. V., Rignot, E., Rippin, D. M., Rivera, A., Roberts, J., Ross, N., Siegert, M. J., Smith, A. M., Steinhage, D., Studinger, M., Sun, B., Tinto, B. K., Welch, B. C., Wilson, D., Young, D. A., Xiangbin, C., and Zirizzotti, A. (2013): Bedmap2: improved ice bed, surface and thickness datasets for Antarctica, The Cryosphere, 7, 375-393, doi:10.5194/tc-7-375-2013.

Gao, F., He, T., Wang, Z., Ghimire, B., Shuai, Y., Masek, J., Schaaf, C. & Williams, C. (2014): Multiscale climatological albedo look-up maps derived from moderate resolution imaging spectrocradiometer BRDF/albedo products. Journal of Applied Remote Sensing. 083532-1, Vol. 8

GLCC v2 (2000): Global Land Cover Characteristics Data Base Version 2.0 (Available at ftp://edcftp.cr.usgs.gov/data/glcc/globdoc2_0.html, last accessed July 2015.).

GLOBCOVER 2009 : Products Description and Validation Report, (2011), ESA Technical Note. ,(Available http://due.esrin.esa.int/files/GLOBCOVER2009_Validation_Report_2.2.pdf, last accessed July 2015.).

GTOPO30 (1996): GTOPO30 - Global Topographic Data, U.S. Geological Survey, EROS Data Center Distributed Active Archive Center (EDC DAAC), Available at https://lta.cr.usgs.gov/GTOPO30 (last accessed July 2015.), USA.

HWSD (2009): Harmonized World Soil Database Version 1.2 Technical Note, Food and Agric. Organ., Rome (Available at: http://webarchive.iiasa.ac.at/Research/LUC/External-World-soil-database/HTML/).

Houldcroft, Caroline J., , William M. F. Grey, Mike Barnsley, Christopher M. Taylor, Sietse O. Los, and Peter R. J. North, 2009: New Vegetation Albedo Parameters and Global Fields

of Soil Background Albedo Derived from MODIS for Use in a Climate Model. J. Hydrometeor, 10, 183–198. , doi: http://dx.doi.org/10.1175/2008JHM1021.1 Koster, R., and M. Suarez, (1991): A simplified treatment of SiB's land surface albedo parameterization, NASA Tech. Memo. 104538.

Koster, R. and M. Suarez, (1996): Energy and Water Balance Calculations in the Mosaic LSM, NASA Tech. Memo. 104606, Vol. 9.

Koster, R. D., M. J. Suarez, A. Ducharne, M. Stieglitz, and P. Kumar (2000), A catchment-based approach to modeling land surface processes in a general circulation model: 1. Model structure, J. Geophys. Res., 105*(*D20*)*, 24809–24822, *doi:*10.1029/2000JD900327.

Koster, R.D., G. K. Walker, G. J. Collatz, and P. E. Thornton, 2014: Hydroclimatic Controls on the Means and Variability of Vegetation Phenology and Carbon Uptake. J. Climate, 27, 5632–5652. doi: http://dx.doi.org/10.1175/JCLI-D-13-00477.1

MODIS (2008), MOD15A2 v005, NASA EOSDIS Land Processes DAAC, USGS Earth Resources Observation and Science (EROS) Center, Sioux Falls, South Dakota (https://lpdaac.usgs.gov), accessed 07-28-2015, at http://e4ftl01.cr.usgs.gov/MOLT/MOD15A2.005/.

MCD43GF (2014): Gap filled product description. SZN-extended MODIS/Terra+Aqua 30 arc-second global gap-filled snow free BRDF parameters product (Available at: ftp://rsftp.eeos.umb.edu/data02/Gapfilled/readme.pdf, last accessed July 2015.)

Eric G. Moody, Michael D. King, Crystal B. Schaaf, and Steven Platnick (2008): MODIS-Derived Spatially Complete Surface Albedo Products: Spatial and Temporal Pixel Distribution and Zonal Averages. J. Appl. Meteor. Climatol., 47, 2879–2894. doi: http://dx.doi.org/10.1175/2008JAMC1795.1

NRCS Soil Survey Staff, USDA (2012): General Soil Map (STATSGO2) [United States]. Available online at http://websoilsurvey.nrcs.usda.gov/. Last accessed July 2015.

Oleson, K. W., and Co-authors, (2010): Technical description of version 4.0 of the Community Land Model (CLM). NCAR Technical Note NCAR/TN-478+STR., National Center for Atmospheric Research, P. O. Box 3000, Boulder, Colorado, 80307-3000.

Reynolds, C. A., T. J. Jackson, and W. J. Rawls (2000): Estimating soil water-holding capacities by linking the Food and Agriculture Organization Soil map of the world with global pedon databases and continuous pedotransfer functions, Water Resour. Res., 36(12), 36533662, doi:10.1029/2000WR900130.

Sellers, P. J., Y. Mintz, Y. C. Sud, and A. Dalcher, (1986): A simple biosphere model (SiB) for use within general circulation models, J. Atmos. Sci., 43, 505-531.

Sheffield, J., G. Goteti, and E. F. Wood, 2006: Development of a 50-yr high-resolution global dataset of meteorological forcings for land surface modeling, J. Climate, 19 (13), 3088-3111.

Simard, M., N. Pinto, J. B. Fisher, and A. Baccini (2011), Mapping forest canopy height globally with spaceborne lidar, J. Geophys. Res., 116, G04021, doi:10.1029/2011JG001708

Verdin, K.L., and J.P. Verdin (1999): A topographical system for delineation and codification of the Earth's river basins. J. of Hydrology (218), 1-12.

Verdin, K (2013): Final Report: High Resolution Topographic Analysis for GMAO's Catchment LSM, pp21. Available at Global Modeling and Assimilation Office, Code 610.1, NASA/Goddard Space Flight Center, Greenbelt, MD 201771.

APPENDIX A: mkCatchParam Software

```
Usage: mkCatchParam -x nx -y ny -g Gridname -b DL -m MA -l LD -s
     SD -e EASE

-x   Size of longitude dimension of input raster. DEFAULT: 8640
-y   Size of latitude dimension of input raster.  DEFAULT: 4320
-g   Gridname(name of the .til or .rst file without file
     extension)
-b   Position of the dateline in the first grid box (DC or DE).
     DEFAULT: DC
-l   Choice of LAI data set (Default MODGEO)
     MODGEO: MODIS with GEOLAND2 overlaid on South America,
          Africa and Australia
     GEOLAND2: 10-day climatology from the period 1999-2011 on
          40320×20160 grid
     GSWP2: Monthly climatology from the period 1982-1998
          on 360×180 grid
     MODIS: 8-day climatology from the period 2000-2013  on
          43200×21600 grid
     GSWPH: Monthly climatology from the 2D-spatially
          interpolated GSWP-2 LAI for the period 1982-1998 on
          43200×21600 grid
-s   Choice of soil data (Default HWSD)
     HWSD: Merged HWSD1.21-STATSGO2 soil properties on
          43200×21600 grid, with De Lannoy (2014) soil hydraulic
          parameters
     NGDC : Reynolds soil texture classes on 4320×2160 grid with
          GSWP2 soil hydraulic  parameters
-m   Choice of MODIS Albedo data (Default MODIS2)
     MODIS1: 16-day Climatology from 1'×1'(21600×10800) MODIS
          data from the period 2000-2004
     MODIS2: 8-day Climatology from 0.5'x0.5'(43200×21600) MODIS
          data from the period 2001-2011
-e   EASE: This option is only used for SMAP grids
```

APPENDIX B: Miscellaneous programs

```
(B1)Deriving parameters for user-specified quasi-rectangular
     grid cells (for e.g., LIS, GSWP-2) either globally or over
     a small domain

USAGE : bin/mkLISTilesPara -vfile VectorFile
```

The user-specified ASCII file (VectorFile) should contain a one-line header followed by latitude and longitude at the center of each grid cell in a row separately for each grid cell. The one-line header reads:

N_Cells, dx,dy, DL, NC_domain,NR_domain, i_offset, j_offset

where:

Four mandatory parameters:

N_Cells number of grid cells in the study
dx cell resolution in longitudinal direction in degrees
dy cell resolution in latitudinal direction in degrees
DL Location of the dateline
0: the dateline lies along the center of the 1st column (for e.g., DC in GEOS-5 finite volume grids)
1: the dateline is along the western edge of the grid

Four optional parameters:

NC_domain* Number of columns in the domain
NR_domain* Number of rows in the domain
i_offset* i index of the lower left grid cell of the domain minus 1 when the domain grid is overlaid on a global grid of the same resolution counting columns from the dateline to the dateline
j_offset* j index of the lower left grid cell of the domain minus 1 when the domain grid is overlaid on a global grid of the same resolution counting rows from the south pole to the north pole

* Note that the last four optional parameters are only used to derive parameters for a smaller rectangular study domain. They must be left blank if parameters are being derived for quasi-rectangular surface elements on a global grid. Note also that if the domain expands to the globe, the expanded grid must have the dateline and the south pole as the western and southern edges.

(B2)Deriving parameter files for SMAP-EASE grids

USAGE : bin/mkSMAPTiles_v2 -smap_grid MXX
Allowed SMAP grids are: M01 M03 M09 M36

(3) Software to debug parameters Section 7.2.4

This utility helps debug the curve-fitting algorithm that derives ars1, ars2, ars3, ara1,ara2, ara3, ara4, arw1, arw2, arw3, arw4 in Section 7.2.4.

```
Usage : chk_clsm_params -s Y -m MaskFile

 -m GEOS5_10arcsec_mask.nc for new mask or just -m for older
     mask

The user will be asked to enter statistics regarding the
     compound topographic index and the soil hydraulic
     properties in the problematic catchment surface element.
     The hope is that no one will ever need to use this
     software. The user is advised to consult the GMAO land
     modeling team should a curve-fitting problem ever arise
     (rather than attempting to debug the problem himself or
     herself).
```

APPENDIX C: Acronyms

AGCM	Atmospheric General Circulation Model
AVHRR	Advanced Very High Resolution Radiometer
BCSDIR	Boundary conditions directory as specified in gcm_run.j in the GEOS-5 experiment
BCRSLV	Resolution as specified in gcm_run.j
CLM	Common Land Model
CLSM	Catchment Land Surface Model
DEM	Digital Elevation Model
ESA	European Space Agency
GEOS-5	Goddard Earth Observing System version 5
GMAO	Global Modeling and Assimilation Office
GrnFrac	Greenness Fraction
GSWP2	The second phase of the Global Soil Wetness Project
HWSDv1.21	Harmonized World Soil Data version 1.21
HYDRO1k	Global coverage of stream and drainage basins derived using USGS 30 arc-second digital elevation model (DEM)
IGBP	International Geosphere Biosphere Project

LAI	Leaf Area Index
LBCs	Land surface Boundary Conditions
MERRA	Modern Era Retrospective analyses for Research and Applications
MODIS	Moderate Resolution Imaging Spectroradiometer
NDVI	Normalized Difference Vegetation Index
NIRDF	Near-infrared Diffused Albedo
NTILES	Number of catchment tiles (surface elements) that make up the Earth's land surface in the data set
SiB2	Simple Biosphere model version 2
SMAP	NASA Soil Moisture Active Passive mission
SRTM	Shuttle Radar Topography Mission
STATSGO2	The Digital General Soil Map of the United States
UCAR	University Corporation for Atmospheric Research
USGS	Unites State Geological Survey
VISDF	Visible Diffused Albedo

APPENDIX D: ACKNOWLEDGEMENTS

Dr. Crystal Schaaf at the University of Massachusetts, Boston provided MODIS BRDF/Albedo CMG Gap-Filled Snow-Free Product MCD43GF V005 data. The authors gratefully acknowledge Clara Draper and Manuella Girotto from the land data assimilation group for their support and insightful feedback during parameter evaluation. Special thanks go to Richard Cullather from the glaciers group for his help in overlaying glaciers onto the mask file.

Previous Volumes in This Series

Volume 1 *September 1994*	Documentation of the Goddard Earth Observing System (GEOS) general circulation model - Version 1 **L.L. Takacs, A. Molod, and T. Wang**
Volume 2 *October 1994*	Direct solution of the implicit formulation of fourth order horizontal diffusion for gridpoint models on the sphere **Y. Li, S. Moorthi, and J.R. Bates**
Volume 3 *December 1994*	An efficient thermal infrared radiation parameterization for use in general circulation models **M.-D. Chou and M.J. Suarez**
Volume 4 *January 1995*	Documentation of the Goddard Earth Observing System (GEOS) Data Assimilation System - Version 1 **James Pfaendtner, Stephen Bloom, David Lamich, Michael Seablom, Meta Sienkiewicz, James Stobie, and Arlindo da Silva**
Volume 5 *April 1995*	Documentation of the Aries-GEOS dynamical core: Version 2 **Max J. Suarez and Lawrence L. Takacs**
Volume 6 *April 1995*	A Multiyear Assimilation with the GEOS-1 System: Overview and Results **Siegfried Schubert, Chung-Kyu Park, Chung-Yu Wu, Wayne Higgins, Yelena Kondratyeva, Andrea Molod, Lawrence Takacs, Michael Seablom, and Richard Rood**
Volume 7 *September 1995*	Proceedings of the Workshop on the GEOS-1 Five-Year Assimilation **Siegfried D. Schubert and Richard B. Rood**
Volume 8 *March 1996*	Documentation of the Tangent Linear Model and Its Adjoint of the Adiabatic Version of the NASA GEOS-1 C-Grid GCM: Version 5.2 **Weiyu Yang and I. Michael Navon**
Volume 9 *March 1996*	Energy and Water Balance Calculations in the Mosaic LSM **Randal D. Koster and Max J. Suarez**
Volume 10 *April 1996*	Dynamical Aspects of Climate Simulations Using the GEOS General Circulation Model **Lawrence L. Takacs and Max J. Suarez**
Volume 11 *May 1997*	Documentation of the Tangent Linear and its Adjoint Models of the Relaxed Arakawa-Schubert Moisture Parameterization Package of the NASA GEOS-1 GCM (Version 5.2) **Weiyu Yang, I. Michael Navon, and Ricardo Todling**
Volume 12 *August 1997*	Comparison of Satellite Global Rainfall Algorithms **Alfred T.C. Chang and Long S. Chiu**
Volume 13 *December 1997*	Interannual Variability and Potential Predictability in Reanalysis Products **Wie Ming and Siegfried D. Schubert**

Volume 14
August 1998
A Comparison of GEOS Assimilated Data with FIFE Observations
Michael G. Bosilovich and Siegfried D. Schubert

Volume 15
June 1999
A Solar Radiation Parameterization for Atmospheric Studies
Ming-Dah Chou and Max J. Suarez

Volume 16
November 1999
Filtering Techniques on a Stretched Grid General Circulation Model
Lawrence Takacs, William Sawyer, Max J. Suarez, and Michael S. Fox-Rabinowitz

Volume 17
July 2000
Atlas of Seasonal Means Simulated by the NSIPP-1 Atmospheric GCM
Julio T. Bacmeister, Philip J. Pegion, Siegfried D. Schubert, and Max J. Suarez

Volume 18
December 2000
An Assessment of the Predictability of Northern Winter Seasonal Means with the NSIPP1 AGCM
Philip J. Pegion, Siegfried D. Schubert, and Max J. Suarez

Volume 19
July 2001
A Thermal Infrared Radiation Parameterization for Atmospheric Studies
Ming-Dah Chou, Max J. Suarez, Xin-Zhong, and Michael M.-H. Yan

Volume 20
August 2001
The Climate of the FVCCM-3 Model
Yehui Chang, Siegfried D. Schubert, Shian-Jiann Lin, Sharon Nebuda, and Bo-Wen Shen

Volume 21
September 2001
Design and Implementation of a Parallel Multivariate Ensemble Kalman Filter for the Poseidon Ocean General Circulation Model
Christian L. Keppenne and Michele M. Rienecker

Volume 22
August 2002
Coupled Ocean-Atmosphere Radiative Model for Global Ocean Biogeochemical Models
Watson W. Gregg

Volume 23
November 2002
Prospects for Improved Forecasts of Weather and Short-term Climate Variability on Subseasonal (2-Week to 2-Month) Time Scales
Siegfried D. Schubert, Randall Dole, Huang van den Dool, Max J. Suarez, and Duane Waliser

Volume 24
July 2003
Temperature Data Assimilation with Salinity Corrections: Validation for the NSIPP Ocean Data Assimilation System in the Tropical Pacific Ocean, 1993–1998
Alberto Troccoli, Michele M. Rienecker, Christian L. Keppenne, and Gregory C. Johnson

Volume 25
December 2003
Modeling, Simulation, and Forecasting of Subseasonal Variability
Duane Waliser, Siegfried D. Schubert, Arun Kumar, Klaus Weickmann, and Randall Dole

Volume 26
April 2005
Documentation and Validation of the Goddard Earth Observing System (GEOS) Data Assimilation System – Version 4
Senior Authors: S. Bloom, A. da Silva and D. Dee

Contributing Authors: M. Bosilovich, J-D. Chern, S. Pawson, S. Schubert, M. Sienkiewicz, I. Stajner, W-W. Tan, and M-L. Wu

Volume 27
December 2008

The GEOS-5 Data Assimilation System - Documentation of Versions 5.0.1, 5.1.0, and 5.2.0.
M.M. Rienecker, M.J. Suarez, R. Todling, J. Bacmeister, L. Takacs, H.-C. Liu, W. Gu, M. Sienkiewicz, R.D. Koster, R. Gelaro, I. Stajner, and J.E. Nielsen

Volume 28
April 2012

The GEOS-5 Atmospheric General Circulation Model: Mean Climate and Development from MERRA to Fortuna
Andrea Molod, Lawrence Takacs, Max Suarez, Julio Bacmeister, In-Sun Song, and Andrew Eichmann

Volume 29
May 2012

Atmospheric Reanalyses – Recent Progress and Prospects for the Future. A Report from a Technical Workshop, April 2010
Michele M. Rienecker, Dick Dee, Jack Woollen, Gilbert P. Compo, Kazutoshi Onogi, Ron Gelaro, Michael G. Bosilovich, Arlindo da Silva, Steven Pawson, Siegfried Schubert, Max Suarez, Dale Barker, Hirotaka Kamahori, Robert Kistler, and Suranjana Saha

Volume 30
September 2012

The GEOS-ODAS, description and evaluation
Guillaume Vernieres, Michele M. Rienecker, Robin Kovach and Christian L. Keppenne

Volume 31
March 2013

Global Surface Ocean Carbon Estimates in a Model Forced by MERRA
Watson W. Gregg, Nancy W. Casey and Cecile S. Rousseaux

Volume 32
March 2014

Estimates of AOD Trends (2002-2012) over the World's Major Cities based on the MERRA Aerosol Reanalysis
Simon Provencal, Pavel Kishcha, Emily Elhacham, Arlindo M. da Silva, and Pinhas Alpert

Volume 33
August 2014

The Effects of Chlorophyll Assimilation on Carbon Fluxes in a Global Biogeochemical Model
Cécile S. Rousseaux and Watson W. Gregg

Volume 34
September 2014

Background Error Covariance Estimation using Information from a Single Model Trajectory with Application to Ocean Data Assimilation into the GEOS-5 Coupled Model
Christian L. Keppenne, Michele M. Rienecker, Robin M. Kovach, and Guillaume Vernieres

Volume 35
December 2014

Observation-Corrected Precipitation Estimates in GEOS-5
Rolf H. Reichle and Qing Liu

Volume 36
March 2015

Evaluation of the 7-km GEOS-5 Nature Run
Ronald Gelaro, William M. Putman, Steven Pawson, Clara Draper, Andrea Molod, Peter M. Norris, Lesley Ott, Nikki Prive, Oreste Reale, Deepthi Achuthavarier, Michael Bosilovich,

Virginie Buchard, Winston Chao, Lawrence Coy, Richard Cullather, Arlindo da Silva, Anton Darmenov, Ronald M. Errico, Marangelly Fuentes, Min-Jeong Kim, Randal Koster, Will McCarty, Jyothi Nattala, Gary Partyka, Siegfried Schubert, Guillaume Vernieres, Yuri Vikhliaev, and Krzysztof Wargan

Volume 37
March 2015

Maintaining Atmospheric Mass and Water Balance within Reanalysis
Lawrence L. Takacs, Max Suarez, and Ricardo Todling

Volume 38
September 2015

The Quick Fire Emissions Dataset (QFED) – Documentation of versions 2.1, 2.2 and 2.4
Anton S. Darmenov and Arlindo da Silva